(a) Determine the equation satisfied by the eigenfrequencies of TM modes that can propagate along the glass.

(b) A plane polarised wave of frequency ω is incident on the glass at an angle α with its magnetic field parallel to the surface of the glass. Determine the amplitude of the reflected wave.

6.9 Determine the near field of a time harmonic electric dipole, and show that both the electric and magnetic fields are of $O(r^{-3})$. Show that this is equivalent to the field of a static electric dipole due to charges q_0 and $-q_0$ at $(0,0,0)$ and $(0,0,l)$.

6.10 Determine the far field of two identical time harmonic electric dipoles with moments in the same direction, separated by a distance, $d > 0$. Describe the far field when (i) $\omega d/c_0 \ll 1$, (ii) $\omega d/c_0 \gg 1$.

6.11 Consider the half wavelength antenna with a piecewise linear current distribution, given by (6.118). Show that the gain is proportional to

$$\frac{\sin^2\theta}{\cos^4\theta}\left\{1-\cos\left(\frac{1}{2}\pi\cos\theta\right)\right\}^2,$$

and that the ratio of its radiation resistance to that when the current distribution is given by (6.110) is

$$\frac{64}{\pi^4}\left(\int_0^\pi \frac{\sin^3\theta}{\cos^4\theta}\left\{1-\cos\left(\frac{1}{2}\pi\cos\theta\right)\right\}^2\right)d\theta \Big/ \int_0^\pi \frac{\cos^2\left(\frac{1}{2}\pi\cos\theta\right)}{\sin\theta}d\theta.$$

Evaluate this ratio numerically using the trapezium rule, and hence show that the radiation resistance only differs by about 1% between these two approximations.

Part two

Nonlinear Waves

So far we have studied only *linear* wave systems. With the exception of electromagnetic waves, we formulated the governing equations by looking at small amplitude disturbances of steady states – a string in equilibrium, a motionless ideal gas or elastic solid, the flat, undisturbed surface of a fluid or solid. If $\mathbf{y}_1$ and $\mathbf{y}_2$ are solutions of a linear system of equations, then $a_1\mathbf{y}_1 + a_2\mathbf{y}_2$ is also a solution for any constants a_1 and a_2. In particular, this means that separation of variables and integral transform methods allow us to determine the solution. In fact, these are the only techniques we have used. Compare what happens for **nonlinear** systems, for example, disturbances of a steady state that do not have a small amplitude. If $\mathbf{y}_1$ and $\mathbf{y}_2$ is a solution of a nonlinear system of equations, then, in general, neither $\mathbf{y}_1 + \mathbf{y}_2$ nor $k\mathbf{y}_1$, with k a constant, are solutions. Our standard mathematical techniques fail, and we must think again.

We begin by introducing some of the techniques that can be used to study nonlinear systems of equations by looking at some specific examples in chapter 7. In section 7.1 we study in detail a simple model for the flow of traffic. The governing equation determines how the density of cars changes along a road with a single lane. In chapter 3 we studied small amplitude disturbances to a compressible gas. In section 7.2 we investigate finite amplitude disturbances. The system of equations has three dependent variables, velocity, density and pressure. Each of these systems can be studied in terms of **characteristic curves**, which carry information from the initial conditions forward in time in a sense that we shall explain below. Another generic feature of these systems is that **shock waves** can form, and we devote some time to investigating their properties.

We have already derived the governing equations for shallow water

waves. The system has two dependent variables, water depth and horizontal velocity, and we begin chapter 8 by considering nonlinear waves on shallow water. After studying Stokes' expansion for weakly nonlinear progressive gravity waves on deep water, we move on to look at how, in shallow water, the nonlinear steepening of water waves can be balanced by the effects of linear dispersion, as expressed by the KdV equation. This is a nonlinear equation, and we examine its wave solutions, known as cnoidal waves. The KdV equation also has a family of solitary wave solutions, which we will consider in detail in section 12.1. We also show how we can use complex variable theory to derive some exact solutions for nonlinear capillary waves.

In chapter 9 we study chemical and electrochemical waves. Chemical waves arise from a self-sustained balance between the tendency of molecular diffusion to smear out distributions of chemicals and limit the maximum concentration, and the tendency of certain reactions to cause the maximum chemical concentration to rise. We end the chapter by considering how we can model the propagation of nerve impulses – an example of an electrochemical wave.

In all of these systems we are interested in how the effect of a nonlinear process (for example, wave steepening or chemical reaction) is modified by that of a linear process (for example, diffusion or dispersion). In general, we find that the result is a coherent, propagating structure (a shock, a soliton or a chemical wave), sustained by a balance between the opposing effects of the linear and nonlinear processes.

7

The Formation and Propagation of Shock Waves

In this chapter we consider various physical systems in which shock waves arise. These systems can be studied in terms of characteristic curves, on which information from the boundary and initial conditions propagates. However, this approach usually only gives a valid solution for a finite time, after which the solution at some points becomes multi-valued. This difficulty can be dealt with by inserting discontinuities in the solution, which represent shock waves.

7.1 Traffic Waves

Traffic flow modelling has developed rapidly over the last forty years, and sophisticated models are used in the planning of new roads and analysis of existing road networks. The type of model that we will discuss is the simplest possible and was one of the first to be postulated. In spite of this, it manages to capture many of the qualitative and quantitative features of real traffic flows. It is an excellent way of introducing the mathematics and physics of shock waves, and the solutions can be readily interpreted in terms of our everyday experience of road travel.

7.1.1 Derivation of the Governing Equation

We begin by stating our main assumptions.

— **There is only one lane of traffic and no overtaking**. This may seem restrictive, but the inclusion of several lanes with traffic switching between lanes, along with a model for overtaking, is a difficult business. Moreover, the model that we will develop has been shown to be in reasonable agreement with observations, even for multi-lane roads

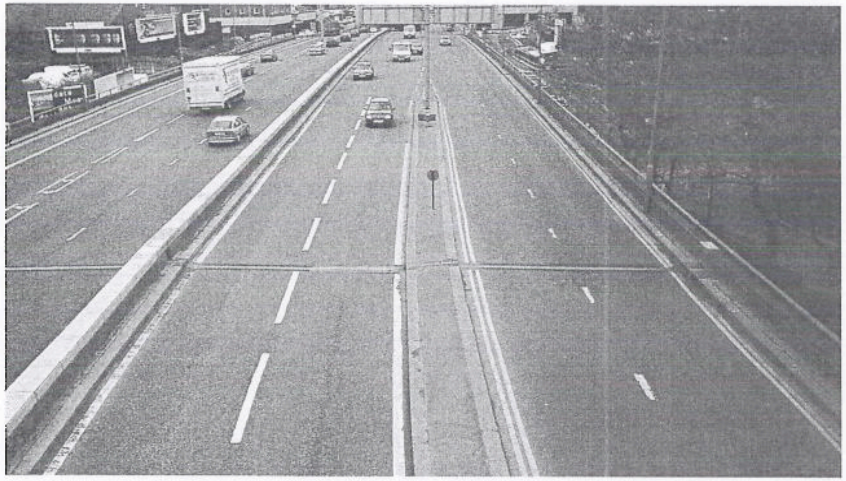

Fig. 7.1. Bunching in lines of traffic.

(see however Kerner (1999) for an introduction to more complex phenomena on multi-lane roads).

— **We can define a local car density, ρ, as the number of cars per unit length of road**. Formally, we are invoking the continuum approximation, which is the basis of fluid mechanics. In fluid mechanics, we do not want to analyse the motion of every fluid molecule, so, at any point, we take a small but finite averaging volume surrounding the point in question, and define the mean density in this volume to be the effective density at the point. In traffic flow modelling, at any point we take a small but finite length of road and define the car density to be proportional to the number of cars within it. Of course, small in this context means something rather different from what it means in fluid mechanics, but the idea is the same. We end up with a function, $\rho(x,t)$, which is defined for every position x and time t.

— **The local car velocity, $v(x,t)$, is a function of the local car density alone ($v \equiv v(\rho)$)**. The underlying idea is that the velocity at which a car is driven is dependent only on the distance from the car in front, and hence on the local car density. This is perhaps the most unrealistic assumption in the model, and we shall see later that we need to modify it.

Now consider a finite length of road, $x_1 \le x \le x_2$. The rate of change of the number of cars in this interval is equal to the flux of cars in at x_1 minus the flux of cars out at x_2, or

$$\frac{\partial}{\partial t}\int_{x_1}^{x_2} \rho(x,t)\,dx = q(x_1,t) - q(x_2,t), \tag{7.1}$$

where $q(x,t)$ is the car flowrate. In terms of ρ and v,

$$q = \rho v(\rho). \tag{7.2}$$

Equation (7.1) is the integral expression for conservation of cars, and must hold for any x_1 and x_2. Notice that there are no x-derivatives, a fact that will prove useful later.

For continuous densities, we can take the limit $x_2 \to x_1$ and obtain the more familiar, differential form for conservation of cars as

$$\frac{\partial \rho}{\partial t} + \frac{\partial q}{\partial x} = 0. \tag{7.3}$$

This is just the one-dimensional version of the generic conservation equation

$$\frac{\partial \mathbf{a}}{\partial t} + \nabla \cdot \mathbf{q} = 0,$$

where $\mathbf{a}$ is a vector whose components are the densities of all the conserved quantities and $\mathbf{q}$ their fluxes. Equation (7.3) is the canonical form for **kinematic waves**. These are waves that arise purely because of the need to conserve mass, or here cars. No force balance is involved, which distinguishes kinematic waves from **dynamic waves**.

The next issue to be addressed is the functional form of $v(\rho)$. We assume that:

— There is an upper limit, $\rho_{\max}$, on the possible density of cars, corresponding to bumper-to-bumper traffic, so that $v(\rho_{\max}) = 0$.

— As the car density increases, drivers slow down. We assume that $v(\rho)$ decreases monotonically for $0 \le \rho \le \rho_{\max}$. Note that traffic flows in the positive x-direction.

As an example, consider figure 7.2, which shows car density and flowrate plotted against car velocity for a real road. The data comes from the M25 motorway between junctions 13 and 14, Britain's busiest stretch of road. Each data point represents an average over one minute between 7 a.m. and 7 p.m. on a weekday. Also shown is a straight line fit to the density data, and the corresponding fitted flowrate. The maximum flowrate lies at around 45 miles per hour, considerably slower than the speed limit of 70 miles per hour. The highest flowrate of cars can be achieved at this

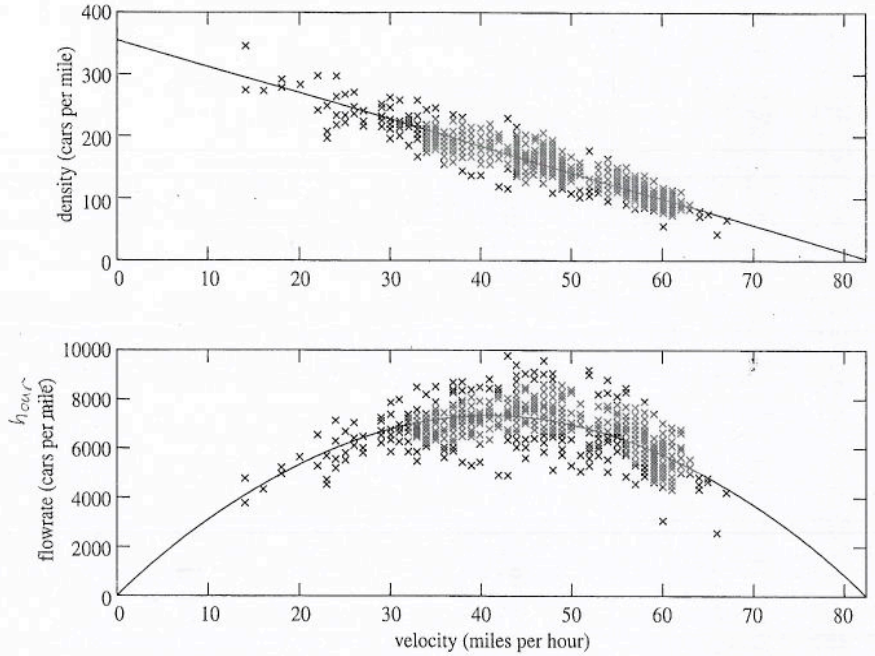

Fig. 7.2. Measured flowrate and density for a stretch of the M25 motorway between 7 a.m. and 7 p.m. on a weekday in 1999. Each data point is an average over one minute.

rather low speed, but with closely packed cars. Indeed, for any density greater than about 200 cars per mile, a higher flowrate can be obtained if everyone slows down and reduces their distance from the car in front.

7.1.2 Small Amplitude Disturbances of a Uniform State

Before studying the full nonlinear problem, it is prudent to consider briefly the linearised model that governs the propagation of small disturbances to a uniform flow of traffic.

By using the chain rule on the x-derivative, we can write (7.3) as

$$\frac{\partial \rho}{\partial t} + c(\rho)\frac{\partial \rho}{\partial x} = 0, \tag{7.4}$$

where

$$c(\rho) = \frac{d}{d\rho}(\rho v) = v(\rho) + \rho v'(\rho) \tag{7.5}$$

is the **kinematic wave speed**. We now look for solutions that are small

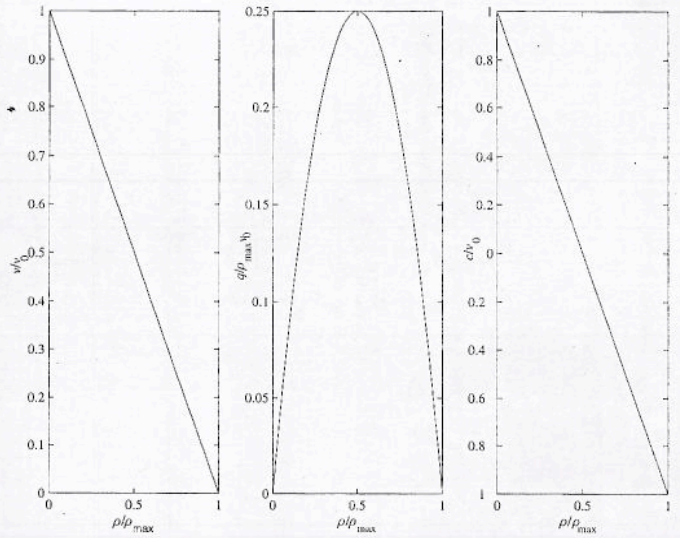

Fig. 7.3. The car velocity, flux function and kinematic wave speed given by (7.14).

amplitude disturbances of a uniform state $\rho = \rho_0$, where ρ_0 is a constant. By writing

$$\rho = \rho_0 + \tilde{\rho}, \quad \text{with } \tilde{\rho} \ll 1, \tag{7.6}$$

and linearising (7.4) we obtain

$$\frac{\partial \tilde{\rho}}{\partial t} + c(\rho_0)\frac{\partial \tilde{\rho}}{\partial x} = 0. \tag{7.7}$$

If we let $\eta = x - c(\rho_0)t$ and look for solutions $\tilde{\rho}(\eta, t)$, we find that (7.7) becomes $\partial\tilde{\rho}/\partial t = 0$, and hence the general solution is

$$\tilde{\rho} = f(x - c(\rho_0)t)$$

for any function, f. This is a **kinematic wave** that propagates in the positive x-direction without change of form at the kinematic wave speed appropriate to the uniform state, $c(\rho_0)$.

If the maximum value of the flux function, $q(\rho)$ is at $\rho = \rho^*$, then $c > 0$ for $\rho < \rho^*$ and $c < 0$ for $\rho > \rho^*$, as illustrated in figure 7.3 for a simple model that we will study later. This means that kinematic waves propagate in the opposite direction to the traffic flow when $\rho > \rho^*$. This demonstrates that what is propagating is not cars, but disturbances in the medium made up of cars; no cars travel backwards when $c < 0$. You may have experienced this phenomenon on a busy road when a sudden

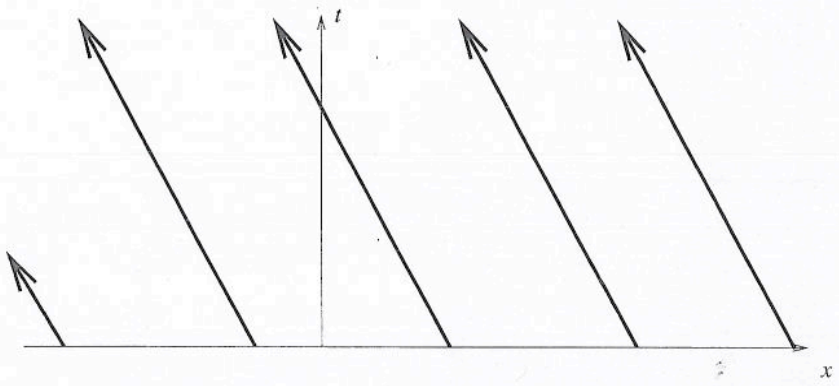

Fig. 7.4. The characteristics for the linearised problem.

increase in car density reaches you from the traffic ahead for no apparent reason.

Kinematic waves occur in many other physical systems. A popular explanation for the dynamics of the spiral arms of galaxies, including our own, is that they are kinematic waves that rotate about the galactic centre, whose underlying medium is interstellar dust and gas. It is not stars that rotate with the arms, but an increased tendency for bright young stars to be born in the high density regions of the wave (see Crosswell (1995)).

Now consider the curves $x = X(t)$ on which ρ is constant. Since the solution propagates at speed $c(\rho_0)$ without change of form, these are just the straight lines

$$x = X(t) = x_0 + c(\rho_0)\, t, \tag{7.8}$$

known as **characteristic curves**, or simply **characteristics**. These are illustrated in figure 7.4 for a case where $c(\rho_0) < 0$. This construction may not seem to be of much use, but we shall see that characteristic curves govern the propagation of the initial car density in the full nonlinear problem.

7.1.3 The Nonlinear Initial Value Problem

We wish to solve

$$\frac{\partial \rho}{\partial t} + c(\rho)\frac{\partial \rho}{\partial x} = 0, \tag{7.9}$$

subject to the initial condition

$$\rho(x, 0) = \rho_0(x). \tag{7.10}$$

Can we construct a set of characteristics, $x = X(t)$, on which ρ is constant, for this nonlinear problem? On these curves

$$\rho(X(t), t) = \rho(X(0), 0) = \rho_0(X(0)),$$

and hence

$$\frac{d}{dt}\{\rho(X(t), t)\} = \frac{\partial \rho}{\partial t} + \frac{dX}{dt}\frac{\partial \rho}{\partial x} = 0.$$

If we compare this expression with (7.9), it is clear that we require

$$\frac{dX}{dt} = c(\rho). \tag{7.11}$$

However, ρ is constant on each characteristic, by definition, so on each characteristic $c(\rho)$ is constant, dX/dt is constant and each characteristic is a straight line given by

$$x = X(t) = x_0 + c(\rho_0(x_0))\, t \quad \text{for } -\infty < x_0 < \infty. \tag{7.12}$$

The solution is given implicitly by (7.12) and

$$\rho(x, t) = \rho_0(x_0). \tag{7.13}$$

This defines the solution, but it is easier to see what is going on by considering a specific problem and examining how the characteristics affect the development of the initial car density profile.

For our example problem, we will use the model

$$v(\rho) = \frac{v_0}{\rho_{\max}}(\rho_{\max} - \rho). \tag{7.14}$$

This is the simplest possible form for the velocity function, consistent with our earlier assumptions about its behaviour, and, as we have seen in figure 7.2, is in reasonable agreement with real data. In this case,

$$c(\rho) = \frac{v_0}{\rho_{\max}}(\rho_{\max} - 2\rho), \tag{7.15}$$

and $\rho^* = \frac{1}{2}\rho_{\max}$; as illustrated in figure 7.3. The initial conditions that we will study are

$$\rho_0(x) = \frac{\rho_L + \rho_R e^{x/L}}{1 + e^{x/L}}, \tag{7.16}$$

for positive constants ρ_L, ρ_R and L. We begin by examining what happens when $\rho_L > \rho_R$. Note that $\rho \to \rho_L$ as $x \to -\infty$ and $\rho \to \rho_R$ as $x \to \infty$, with the change between these two states occurring over a distance of $O(L)$, as illustrated in figure 7.5. We study this simple initial condition to

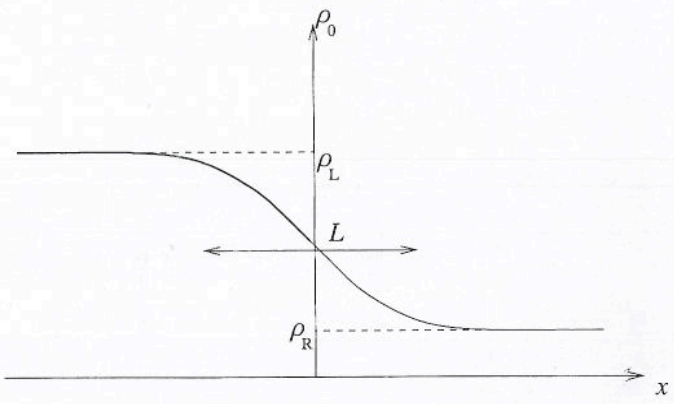

Fig. 7.5. The initial conditions for the initial value problem given by (7.16) with $\rho_L > \rho_R$.

illustrate the fundamental difference between cases where the car density increases with x and those where it decreases.

Since the kinematic wave speed, $c(\rho)$, is a decreasing function of ρ, and the initial conditions have $\rho_0(x)$ a decreasing function of x, $c(\rho_0(x))$ is an increasing function of x, with

$$c(\rho_0(x)) = \frac{v_0}{\rho_{\max}} \left\{ \frac{\rho_{\max} - 2\rho_L + (\rho_{\max} - 2\rho_R)\, e^{x/L}}{1 + e^{x/L}} \right\}, \tag{7.17}$$

as illustrated in figure 7.6. This means that the dX/dt increases as x_0 increases, and hence the characteristics are as illustrated in figure 7.7. There is a unique characteristic through every point in the domain of solution. Qualitatively, the spreading out of the characteristics leads to a spreading out of the initial density profile, as shown in figure 7.8. Note that the solution is sketched in a frame of reference moving to the right at speed $c(\rho_0(0))$, so that the density at the point $x - c(\rho_0(0))t = 0$ remains constant. Each point on the initial profile is shifted to the right by a distance $c(\rho_0(x_0))\,t$. Remember, this does not mean that cars are actually moving with speed $c(\rho_0(x_0))$, simply that a disturbance propagates at this speed. Cars accelerate out of the high density region into the low density region, and the deficit in cars travels backwards. Cars are the molecules that make up the medium whose properties we are studying.

Now consider the initial conditions (7.16) in the limit $L \to 0$, so that

$$\rho_0(x) = \left\{ \begin{array}{ll} \rho_L & \text{for } x < 0, \\ \rho_R & \text{for } x > 0. \end{array} \right\} \tag{7.18}$$

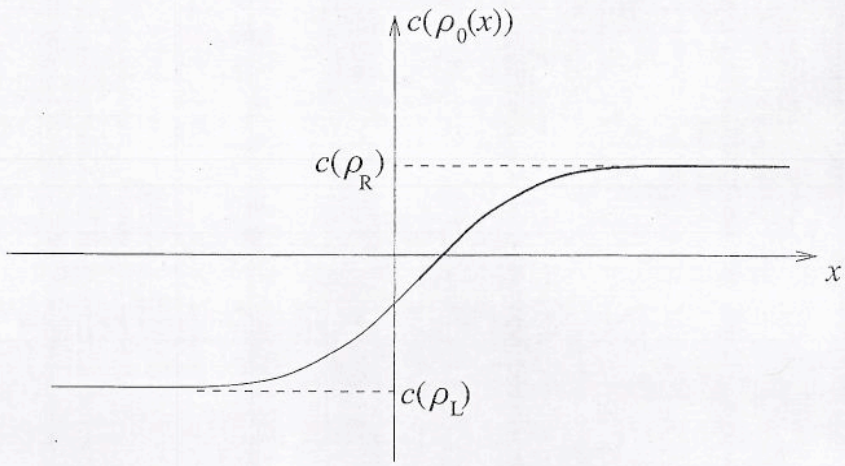

Fig. 7.6. The initial kinematic wave speed for the initial value problem given by (7.16) with $\rho_L > \rho_R$.

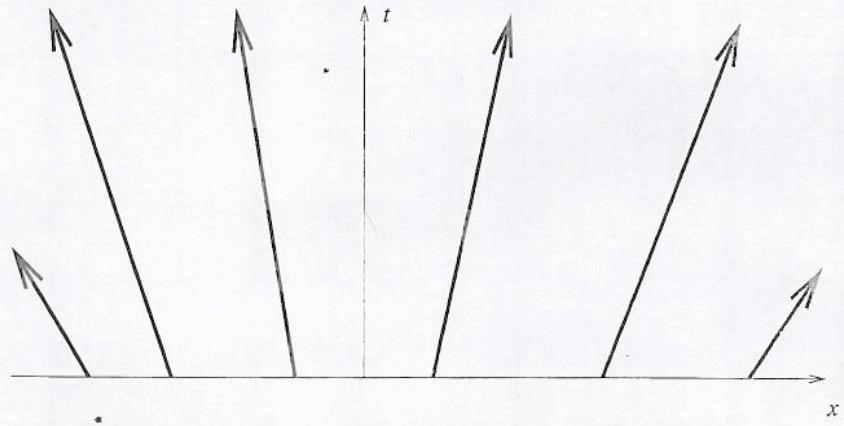

Fig. 7.7. The characteristics for the initial value problem given by (7.16) with $\rho_L > \rho_R$.

The initial value problem given by (7.9) and (7.18) is known as the **Riemann problem**, and is of fundamental importance both for understanding the behaviour of this type of system and for constructing numerical solution schemes (see LeVeque (1990)). The characteristics are given by

$$\left. \begin{array}{ll} x = x_0 + c(\rho_L)\, t, & \text{for } x_0 < 0, \\ x = x_0 + c(\rho_R)\, t, & \text{for } x_0 > 0. \end{array} \right\} \tag{7.19}$$

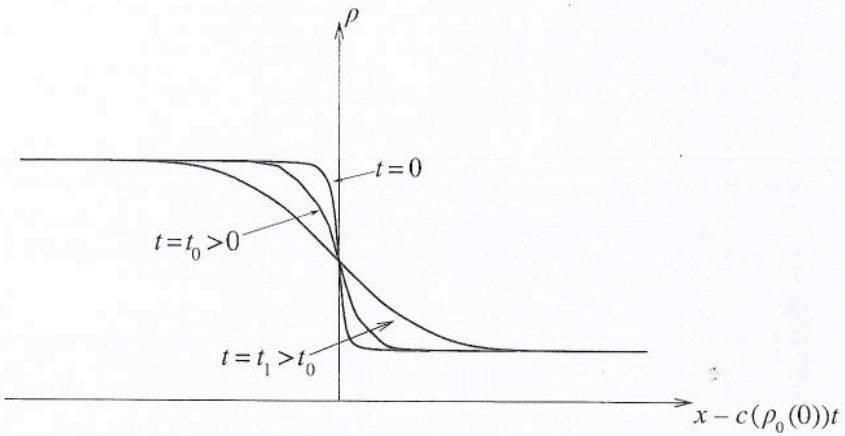

Fig. 7.8. The development of the car density for the initial value problem given by (7.16) with $\rho_L > \rho_R$.

For characteristics that begin at the origin, $x_0 = 0$ and the ratio x_0/L is indeterminate as $L \to 0$. To deal with this we let $x_0 = k_0 L$, where k_0 is a constant. Now $x_0/L = k_0$ for all values of L, and a characteristic beginning at the origin is given by

$$x = \frac{v_0}{\rho_{\max}} \left\{ \frac{\rho_{\max} - 2\rho_L + (\rho_{\max} - 2\rho_R)\, e^{k_0}}{1 + e^{k_0}} \right\} t, \tag{7.20}$$

for any value of k_0. As k_0 varies from $-\infty$ to ∞, this describes a family of straight lines through the origin with $c(\rho_L) < x/t < c(\rho_R)$. A family of characteristics emanating from a single point in this way is known as an **expansion fan**, **expansion wave** or **rarefaction wave**. We can now sketch all of the characteristics in figure 7.9.

To the left of the characteristic $x = c(\rho_L)t$ there is a uniform density $\rho = \rho_L$, whilst to the right of $x = c(\rho_R)t$ there is a uniform density $\rho = \rho_R$. Between these two characteristics the expansion fan solution is given by the characteristic equation itself, $c(\rho) = x/t$. To summarise, the Riemann problem with $\rho_L > \rho_R$ has solution

$$\rho(x,t) = \left\{ \begin{array}{cc} \rho_L & \text{for } x \le c(\rho_L)\, t, \\ \frac{1}{2}\rho_{\max}\left(1 - x/v_0 t\right) & \text{for } c(\rho_L)t \le x \le c(\rho_R)t, \\ \rho_R & \text{for } x \ge c(\rho_R)\, t, \end{array} \right\} \tag{7.21}$$

as shown in figure 7.10. When $\rho_L = \rho_{\max}$ and $\rho_R = 0$, we have the situation that occurs when a traffic light goes green. From an initially stationary line of bumper-to-bumper traffic, the front cars accelerate off

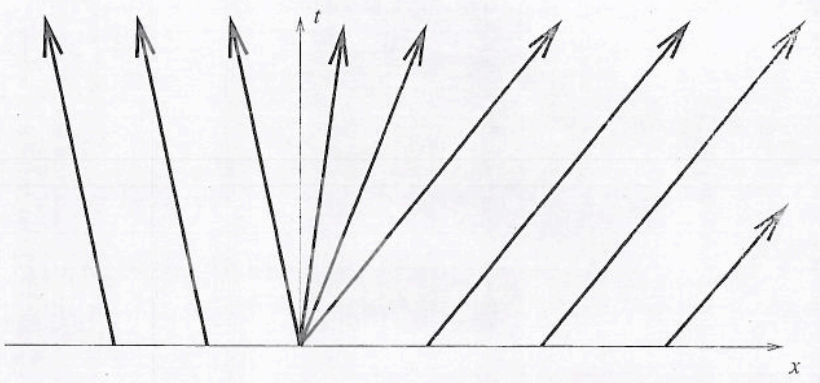

Fig. 7.9. The characteristics for the Riemann problem with $\rho_L > \rho_R$.

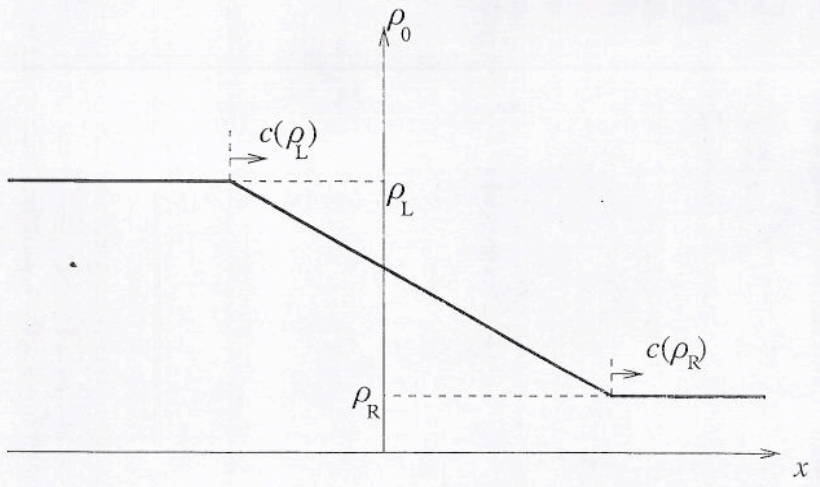

Fig. 7.10. The solution of the Riemann problem with $\rho_L > \rho_R$.

into the clear stretch of road ahead, and the front of the queue spreads out with the effect of the green light propagating back through the traffic at a constant velocity $c(\rho_{\max}) = -v_0$.

At this point, it is worth noting the self-similarity of this solution. The only quantities involved in the Riemann problem are ρ, ρ_L, ρ_R, $\rho_{\max}$, v_0, x and t. There is no geometrical length scale in the problem, so we expect the solution to be a function of some dimensionless combination of the above quantities. The only such combinations are ratios of two densities, and the quantity $x/v_0 t$. This leads us to suspect that the appropriate

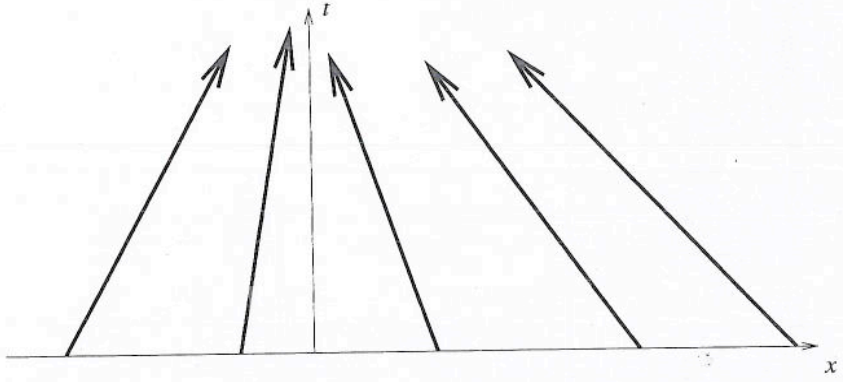

Fig. 7.11. The characteristics for the initial value problem given by (7.16), $\rho_R > \rho_L$.

solution is of the form $\rho = \rho_1 f\left(x/v_0 t\right)$ for some function f and density ρ_1. The solution (7.21) is clearly of this form. In addition, if we substitute this form into (7.9) we find that

$$\left\{\frac{x}{t} - c(\rho)\right\} f'\left(\frac{x}{v_0 t}\right) = 0. \tag{7.22}$$

This means that the solution must consist of spatially uniform sections and expansion fans.

We now consider the apparently equally straightforward case, $\rho_R > \rho_L$. By the converse of the arguments presented above, the kinematic wave speed $c(\rho_0(x))$ is now a decreasing function of x, and hence the characteristics are as shown in figure 7.11. It is clear from the figure that characteristics must eventually intersect. By definition, ρ is constant on each characteristic, so if two intersect, which value of ρ are we to take as the solution? As it stands, our initial value problem becomes ill-posed as soon as any characteristics meet, and we must consider what is missing from our simple model. Before turning to this question we can calculate under what circumstances characteristics will intersect, and where and when this happens.

Consider two characteristics that intersect. Any characteristic that begins at some point between these intersecting characteristics must meet one of them at an earlier time, as shown in figure 7.12, ignoring the unlikely case when *all* the intermediate characteristics intersect at a single point. This means that the earliest intersection must be between neighbouring characteristics. Consider two characteristics, $x = X_1(t)$ and

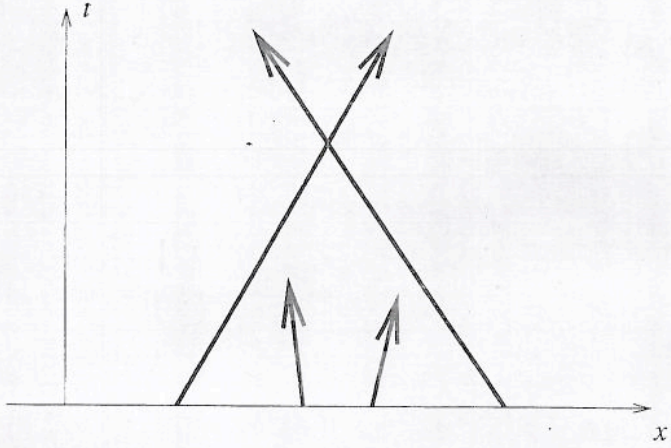

Fig. 7.12. If two characteristics intersect, any enclosed characteristic must meet one of them at an earlier time.

$x = X_2(t)$ given by

$$X_1(t) = x_0 + c(x_0)t,$$
$$X_2(t) = x_0 + \delta x + c(x_0 + \delta x)t.$$

For notational convenience we write $c(x)$ for $c(\rho_0(x))$ here. As $\delta x \to 0$ we obtain neighbouring characteristics, and

$$X_2(t) \approx x_0 + \delta x + c(x_0)t + \delta x c'(x_0)t,$$

where $c'(x) = dc(\rho_0(x))/dx$. If these characteristics intersect at time $t = T$, $X_1(T) = X_2(T)$ and hence

$$T = -\frac{1}{c'(x_0)}.$$

There are two points to be made here:

— If $c'(x_0) > 0$ for $-\infty < x_0 < \infty$, the characteristics never intersect for $t > 0$, and the solution constructed using characteristics is valid everywhere. This is what we found when $\rho_L > \rho_R$.

— If $c'(x_0) < 0$ at *any* point x_0, a pair of characteristics will intersect and the solution as constructed becomes ill-defined. This first occurs when $t = T_{\min}$, where

$$T_{\min} = \min_{-\infty < x_0 < \infty} \left\{-\frac{1}{c'(x_0)}\right\}, \tag{7.23}$$

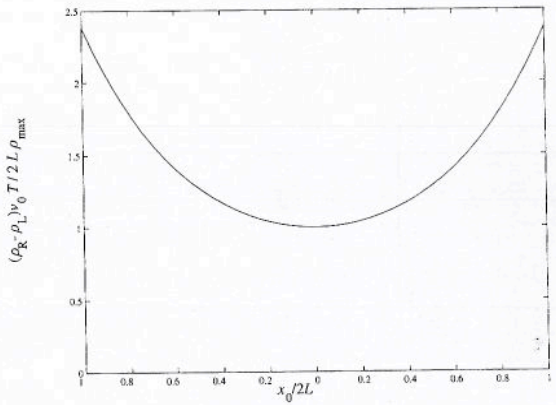

Fig. 7.13. The time, T at which neighbouring characteristics meet for the initial value problem given by (7.16) with $\rho_R > \rho_L$.

in other words, where the initial slope of the car density is most negative. The solution constructed using characteristics is, therefore, valid for $0 \leq t \leq T_{\min}$.

For our particular example, we calculate that

$$T = \frac{2L\rho_{\max}}{(\rho_R - \rho_L)v_0} \cosh^2\left(\frac{x_0}{2L}\right), \tag{7.24}$$

which is sketched in figure 7.13, and hence

$$T_{\min} = \frac{2L\rho_{\max}}{(\rho_R - \rho_L)v_0}, \tag{7.25}$$

with the first intersection of characteristics occurring at $x_0 = 0$. As $t \to T_{\min}$ the density profile steepens until, at $t = T_{\min}$, an infinite slope develops at $x = c(\rho_0(0))T_{\min}$, as shown in figure 7.14. As we have seen, the solution is not valid for $t > T_{\min}$, but we can still sketch what we obtain using the characteristics to construct the solution.

Figure 7.15 shows that the profile overturns and becomes multi-valued. Within this region, there are three characteristics through each point, and hence three possible values of ρ. At the boundaries of this multi-valued region, two neighbouring characteristics meet, and hence the location of the multi-valued region for our example problem can be deduced from (7.24). A typical example is sketched in figure 7.13. The appearance of an infinite slope at $x = 0$ when $t = T_{\min}$ suggests that a **shock wave** is formed. Mathematically, a shock wave is a discontinuity in one or more

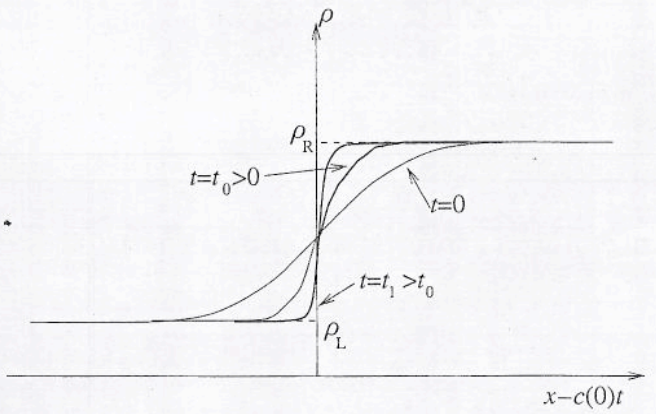

Fig. 7.14. The solution of the initial value problem given by (7.16) with $\rho_R > \rho_L$ for $t \leq T_{\min}$.

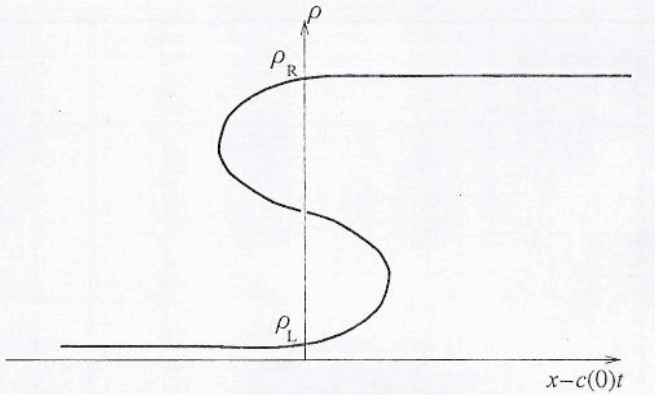

Fig. 7.15. The multi-valued solution of the initial value problem given by (7.16) with $\rho_R > \rho_L$ for $t > T_{\min}$.

of the dependent variables (here there is only one dependent variable). Physically, a shock wave is a thin surface across which one or more of the physical properties changes rapidly and some physical effect, often viscous dissipation, cannot be neglected as it can in the rest of the domain of solution. Before considering what effects we have neglected in our traffic flow model, and whether their inclusion allows us to show that a shock wave actually exists, we can consider where such a shock wave might be located.

Where should we insert a shock wave into the profile shown in figure 7.15? Since our governing equation is an expression of the fact that

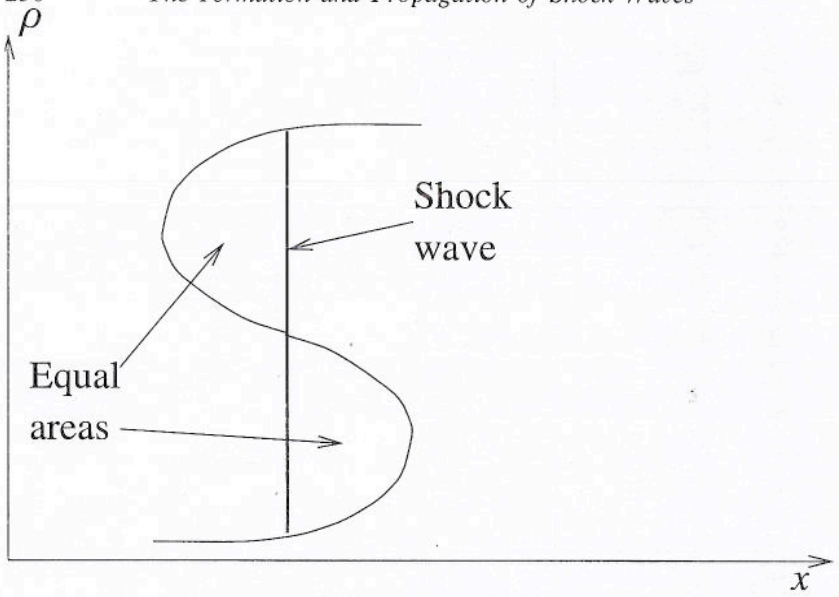

Fig. 7.16. The equal area rule.

the number of cars is preserved, we should insert a discontinuity so as to cut off equal areas in the profile, as shown in figure 7.16. This is known as the **equal area rule**, and using it the number of cars is conserved. Note that this solution satisfies the integral form of car conservation, (7.1). In this form, there are no x-derivatives, and the discontinuity does not cause us a problem. The characteristics and the position of the shock are illustrated in figure 7.17. This procedure is known as **shock fitting**. Note that characteristics enter the shock and then play no further part in the construction of the solution. Consider the case $\rho_R = \rho_{max}$, $\rho_L < \rho_{max}$. This is what happens as cars approach a stationary queue behind a red traffic light. On meeting the queue, cars slow down to a stop, and the lengthening of the queue is achieved through a shock wave propagating backwards.

In section 10.1, we will show how to justify this procedure by introducing some extra physics into the problem, specifically, the reasonable notion that (most) drivers actually look a little further ahead than the bumper of the car in front.

7.1.4 The Speed of the Shock

Now that we have found that shock waves can form, how fast do they move? Consider a shock whose position is given by $x = s(t)$, $\rho = \rho^-$ at

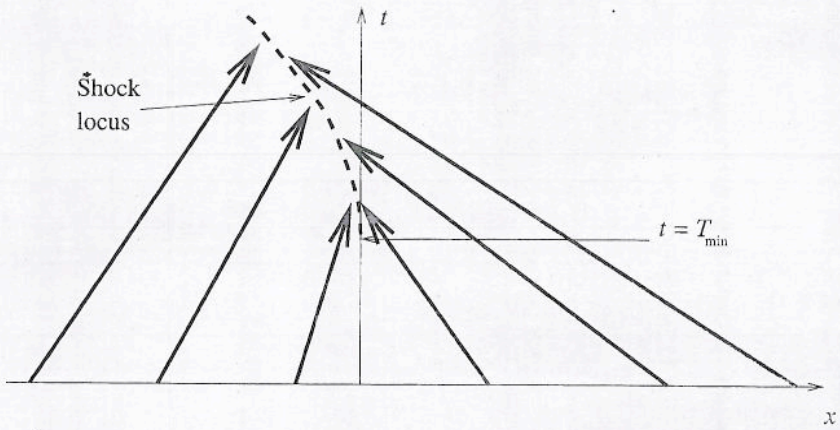

Fig. 7.17. The characteristics and shock locus for the initial value problem given by (7.16) with $\rho_R > \rho_L$.

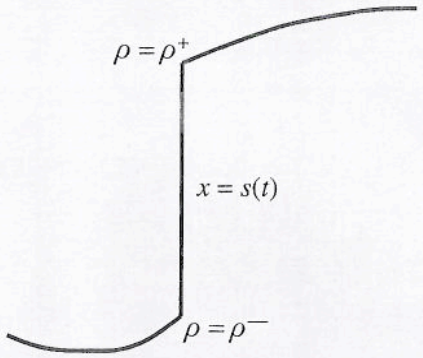

Fig. 7.18. A shock wave.

$x = s^-$, and $\rho = \rho^+$ at $x = s^+$, as sketched in figure 7.18. Conservation of cars in integral form, (7.1), gives

$$\frac{\partial}{\partial t}\left(\int_{x_1}^{s(t)} + \int_{s(t)}^{x_2}\right)\rho(x,t)dx = q(x_1,t) - q(x_2,t),$$

and hence

$$\int_{x_1}^{x_2}\frac{\partial \rho}{\partial t}dx + \frac{ds}{dt}\rho^- - \frac{ds}{dt}\rho^+ = q(x_1,t) - q(x_2,t). \qquad (7.26)$$

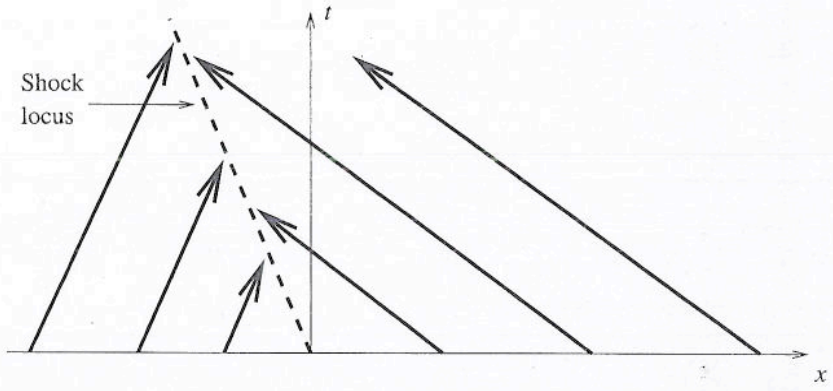

Fig. 7.19. The characteristics and shock locus for the Riemann problem with $\rho_L < \rho_R$.

If we now let $x_2 \to s(t)$ and $x_1 \to s(t)$, the integral vanishes and we are left with

$$q(\rho^-) - \rho^- \frac{ds}{dt} = q(\rho^+) - \rho^+ \frac{ds}{dt},$$

and hence the shock speed is given by

$$\frac{ds}{dt} = \frac{q(\rho^-) - q(\rho^+)}{\rho^- - \rho^+}. \tag{7.27}$$

For the simple case, with $q(\rho) = \rho v(\rho) = \rho v_0(\rho_{\max} - \rho)/\rho_{\max}$, we find that $ds/dt = (v(\rho^-) + v(\rho^+))/2$. As we shall see in section 7.2, this procedure can be generalised to systems of conservation laws.

We can now return, after our lengthy diversion, to our example initial value problem with $\rho_L < \rho_R$. What happens as $L \to 0$? In other words, what is the solution of the Riemann problem when $\rho_L < \rho_R$? Equation (7.23) shows that $T_{\min} \to 0$ as $L \to 0$, so in this limit a shock forms immediately. The initial conditions take the form of a shock wave, and this persists for all time, rather than opening out into an expansion wave as was the case for $\rho_L > \rho_R$. The constant speed of the shock can be calculated from (7.27). The characteristics are illustrated in figure 7.19. Note that all of the characteristics terminate in the shock. Looking back to the case $\rho_L > \rho_R$, we found that the characteristics for the appropriate solution were as shown in figure 7.9. However, we can also construct a shock wave solution of this Riemann problem, with characteristics as shown in figure 7.20. We can exclude this solution by considering the possible travelling wave solutions with $v > 0$ (see section 10.3). Another

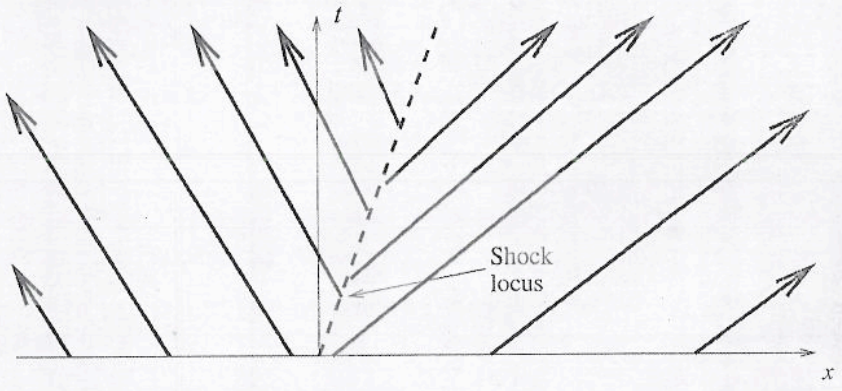

Fig. 7.20. An unphysical shock wave solution of the Riemann problem with $\rho_L > \rho_R$.

way of excluding this solution is by noting that it has characteristics that originate at the shock. This is unphysical, since the solution should depend upon the initial conditions, not on conditions at the shock.

7.2 Compressible Gas Dynamics

In chapter 3 we studied sound waves, which are small amplitude disturbances of a stationary body of compressible gas. In this section we study the dynamics of a compressible gas when the amplitude of the disturbances is not small. In particular, we will find that shock waves can form, and study their properties. Figure 7.21 shows a shadowgraph of the shock waves generated by a fast moving projectile. The pressure, density, velocity and local sound speed in the gas can all change discontinuously across shock waves. An essential preliminary to understanding this is a brief study of the thermodynamics of ideal gases.

7.2.1 Some Essential Thermodynamics

In classical kinetic theory, the **theorem of equipartition of energy** tells us that there is an average internal energy $\frac{1}{2}kT$ associated with every degree of freedom of the molecules in an ideal gas, for which there is no intermolecular attraction, where k is **Boltzmann's constant** and T is the absolute temperature. For an atom in translational motion there are three degrees of freedom, so its internal energy is $\frac{3}{2}kT$. For one mole of these atoms, the energy is $\frac{3}{2}kN_A T$, where N_A is **Avogadro's number**.

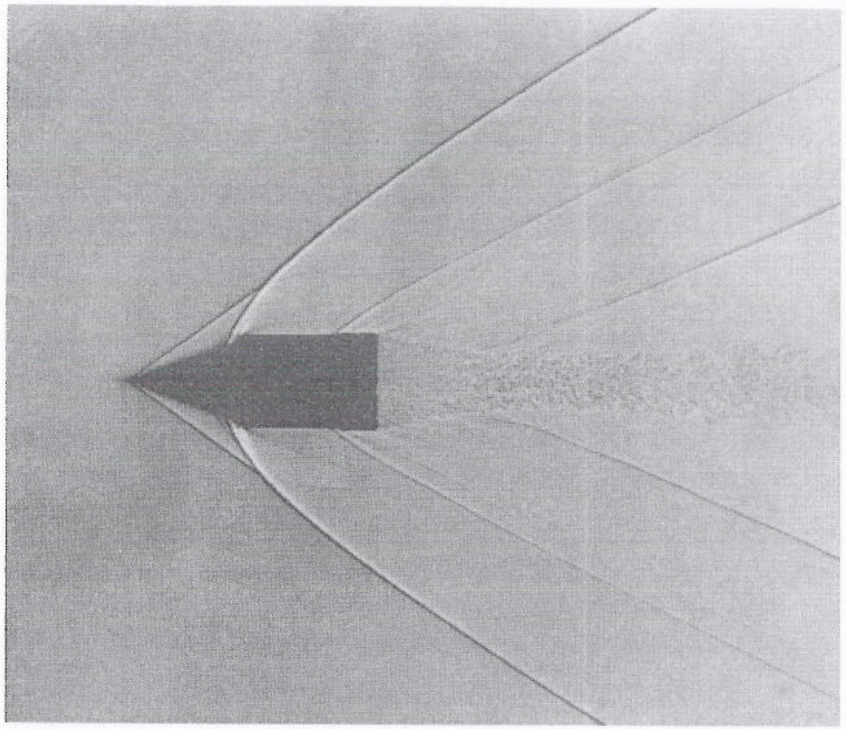

Fig. 7.21. The shock waves generated by a projectile at Mach number $M \approx 1.7$.

The **universal gas constant** is $R = kN_A \approx 8.3\,\mathrm{J\,mol^{-1}\,K^{-1}}$, so the internal energy of a mole of atoms is $E = \frac{3}{2}RT$. For a mole of molecules composed of two atoms, in addition to the translational degrees of freedom there are two further rotational degrees of freedom, so that the total internal energy is $E = \frac{5}{2}RT$. This is a reasonable approximation for air, which consists mainly of the diatomic gases nitrogen and oxygen. Note that E is directly proportional to the absolute temperature in an ideal gas.

Let's now consider the changes in temperature and pressure that occur when a gas is heated and its volume allowed to vary. If an amount of heat Q is absorbed (or given up) by a volume of gas, and the work done in any change of volume is W, then the change in internal energy (which we consider to be reversible) is given by the **first law of thermodynamics**,

$$dE = Q - W. \tag{7.28}$$

If we neglect viscous and magnetic effects, we have $W = pdV$, so that $dE = Q - pdV$.

We now introduce the idea of the **entropy** of a gas, S, as the amount of thermal energy that is unavailable for conversion into mechanical energy. This leads us to regard entropy as a measure of the randomness or disorder in the gas. In particular, if an amount of heat Q is absorbed at an absolute temperature T, then the entropy is increased by an amount $dS = Q/T$, and we can state the **second law of thermodynamics** as

$$dE = TdS - pdV. \tag{7.29}$$

If we now regard E as a function of S and V,

$$dE = \left(\frac{\partial E}{\partial S}\right)_V dS + \left(\frac{\partial E}{\partial V}\right)_S dV,$$

so that we can formally define

$$T = \left(\frac{\partial E}{\partial S}\right)_V, \quad p = -\left(\frac{\partial E}{\partial V}\right)_S.$$

In these equations, the subscript indicates which variable is to be held constant during the differentiation.

There are two further energies that will be of use to us here: the **enthalpy**, $H = E + pV$, and the **free energy**, $F = E - TS$. These are measures of how much energy the gas has available to exchange with its surroundings. Now $dH = dE + pdV + Vdp$, which, using the second law of thermodynamics, (7.29), can be written as

$$dH = TdS + Vdp.$$

Regarding H as a function of S and p, we have

$$T = \left(\frac{\partial H}{\partial S}\right)_p, \quad V = \left(\frac{\partial H}{\partial p}\right)_S.$$

Assuming smoothness of the second partial derivatives of the enthalpy gives

$$\left(\frac{\partial T}{\partial p}\right)_S = \left(\frac{\partial V}{\partial S}\right)_p. \tag{7.30}$$

A similar calculation for the free energy gives

$$\left(\frac{\partial p}{\partial T}\right)_V = \left(\frac{\partial S}{\partial V}\right)_T, \tag{7.31}$$

a result that we will make use of shortly.

If the gas absorbs an amount of heat Q and its temperature rises by dT, we can define the **specific heat** c by the relation $Q = cdT$. The first

law of thermodynamics states that $dE = cdT - pdV$. If this absorption of heat takes place at constant volume, we have $c = c_V$, the **specific heat at constant volume**, and $dE = c_V dT$, $c_V = (\partial E/\partial T)_V$. As we have seen, for a diatomic ideal gas $c_V = \frac{5}{2}R$. If the absorption of heat takes place at constant pressure, $c = c_p$, the **specific heat at constant pressure**, and $dp = 0$, so we have $c_p dT = dE + pdV$, so that

$$c_p = \left(\frac{\partial E}{\partial T}\right)_p + p\left(\frac{\partial V}{\partial T}\right)_p = \left[\frac{\partial}{\partial T}(E + pV)\right]_p = \left(\frac{\partial H}{\partial T}\right)_p,$$

which we can use to derive a relationship between c_p and c_V. If we regard E as a function of $V(p, T)$ and T rather than V and S, then

$$c_p = \left(\frac{\partial H}{\partial T}\right)_p = \frac{\partial}{\partial T}\{E(V(p, T), T) + pV\}$$
$$= \left(\frac{\partial E}{\partial V}\right)_T \left(\frac{\partial V}{\partial T}\right)_p + \left(\frac{\partial E}{\partial T}\right)_V + p\left(\frac{\partial V}{\partial T}\right)_p.$$

This means that

$$c_p = c_V + \left\{\left(\frac{\partial E}{\partial V}\right)_T + p\right\}\left(\frac{\partial V}{\partial T}\right)_p.$$

Now, from the second law of thermodynamics, (7.29),

$$\left(\frac{\partial E}{\partial V}\right)_T = T\left(\frac{\partial S}{\partial V}\right)_T - p,$$

so that

$$c_p = c_V + T\left(\frac{\partial S}{\partial V}\right)_T \left(\frac{\partial V}{\partial T}\right)_p,$$

and from (7.31)

$$c_p = c_V + T\left(\frac{\partial p}{\partial T}\right)_V \left(\frac{\partial V}{\partial T}\right)_p.$$

For one mole of an ideal gas $pV = RT$. Evaluating the partial derivatives

$$\left(\frac{\partial p}{\partial T}\right)_V = \frac{R}{V}, \quad \left(\frac{\partial V}{\partial T}\right)_V = \frac{R}{p},$$

then gives $c_p = c_V + R$. For a diatomic ideal gas, $c_p = \frac{7}{2}R$.

From the second law of thermodynamics, (7.29),

$$dS = c_V \frac{dT}{T} + p\frac{dV}{T} = c_V \frac{dT}{T} + R\frac{dV}{V},$$

and hence

$$\frac{dS}{c_V} = \frac{dT}{T} + \left(\frac{c_p}{c_V} - 1\right)\frac{dV}{V}.$$

If we define $\gamma = c_p/c_V$, the **ratio of specific heats** of the gas, then this relationship is easily integrated to give $TV^{\gamma-1} = Ae^{S/c_V}$ for some constant A. Using the ideal gas law, this gives

$$\frac{S}{c_V} = \log\left(\frac{p}{\rho^\gamma}\right) + \text{constant}, \tag{7.32}$$

and hence

$$p = \kappa e^{S/c_V}\rho^\gamma \tag{7.33}$$

for some constant, κ. For a diatomic ideal gas, $\gamma = 1.4$. This is the equation we used in section 3.1 when we determined the speed of sound in a gas. As we will show below, the entropy of a gas satisfies a very simple equation, and the thermodynamics that we have studied in this section is enough to allow us to investigate the properties of shock waves. It is now clear that the internal energy E of a unit mass of gas can be written as

$$E = c_V T = \frac{p}{(\gamma - 1)\rho}. \tag{7.34}$$

7.2.2 Equations of Motion

We will now assume that the gas is inviscid and that the effect of gravity is negligible, as we did in section 3.1, but we will not assume that the motion of the gas is a small disturbance to a stationary body of gas. It is most convenient to write the equations for the conservation of mass and momentum in the form

$$\frac{D\rho}{Dt} + \rho\nabla\cdot\mathbf{u} = 0, \tag{7.35}$$

$$\frac{D\mathbf{u}}{Dt} + \frac{1}{\rho}\nabla p = 0. \tag{7.36}$$

We now also need the equation for conservation of energy. The energy per unit mass of the gas consists of the internal energy, E, and the kinetic energy, $\frac{1}{2}|\mathbf{u}|^2$. The equation for conservation of energy relates the flux of this energy to the rate of working of the pressure forces and is given by

$$\frac{\partial}{\partial t}\left(\frac{1}{2}\rho|\mathbf{u}|^2 + \rho E\right) + \nabla\cdot\left\{\left(\frac{1}{2}\rho|\mathbf{u}|^2 + \rho E + p\right)\mathbf{u}\right\} = 0. \tag{7.37}$$

This can be rearranged to give

$$\frac{D}{Dt}\left(\frac{1}{2}\rho|\mathbf{u}|^2+\rho E\right)+\left(\frac{1}{2}\rho|\mathbf{u}|^2+\rho E\right)\nabla\cdot\mathbf{u}+\nabla\cdot(p\mathbf{u})=0,$$

and hence

$$\frac{1}{2}|\mathbf{u}|^2\frac{D\rho}{Dt}+\rho\mathbf{u}\cdot\frac{D\mathbf{u}}{Dt}+E\frac{D\rho}{Dt}+\rho\frac{DE}{Dt}+\left(\frac{1}{2}\rho|\mathbf{u}|^2+\rho E\right)\nabla\cdot\mathbf{u}+p\nabla\cdot\mathbf{u}+\mathbf{u}\cdot\nabla p=0.$$

If we now eliminate $\nabla\cdot\mathbf{u}$ and $D\mathbf{u}/Dt$ using (7.35) and (7.36), we obtain

$$\frac{DE}{Dt}-\frac{p}{\rho^2}\frac{D\rho}{Dt}=0.$$

Since we know that

$$T\,dS=dE-pdV=dE-\frac{p}{\rho^2}\,d\rho,$$

we finally arrive at

$$\frac{DS}{Dt}=0.$$

This is the simplest possible way of expressing conservation of energy in an ideal, inviscid flow, and states that entropy is advected with the flow, and hence is constant on streamlines. Physically, this result comes directly from the notion of an ideal gas, where the molecular diffusivity is zero. Consequently, no heat can be transferred between fluid particles, and the entropy must be in thermodynamic equilibrium. This type of flow is said to be **isentropic**. If the entropy is spatially uniform, the flow is said to be **homentropic**. In particular, in a homentropic flow with no shock waves, $S=S_0$, then $p=k\rho^\gamma$, where $k=\kappa e^{S_0/c_v}$ is a constant. This is the relationship between pressure and density that we used in chapter 3. Equations (7.35) and (7.36) become

$$\frac{\partial\rho}{\partial t}+\nabla\cdot(\rho\mathbf{u})=0, \tag{7.38}$$

$$\frac{\partial\mathbf{u}}{\partial t}+\mathbf{u}\cdot\nabla\cdot\mathbf{u}+k\gamma\rho^{\gamma-2}\nabla\rho=0. \tag{7.39}$$

For one-dimensional flows these are

$$\frac{\partial\rho}{\partial t}+\frac{\partial(\rho u)}{\partial x}=0, \tag{7.40}$$

$$\frac{\partial u}{\partial t}+u\frac{\partial u}{\partial x}+k\gamma\rho^{\gamma-2}\frac{\partial\rho}{\partial x}=0. \tag{7.41}$$

7.2.3 Construction of the Characteristic Curves

Can we construct characteristic curves for the system (7.40) and (7.41)? The easiest way to answer this question is to consider the system in terms of u and the local sound speed,

$$c=\left(\frac{\partial p}{\partial\rho}\right)_S^{1/2}=\sqrt{\gamma k\rho^{\gamma-1}}.$$

In terms of c, (7.40) and (7.41) become

$$2\frac{\partial c}{\partial t}+2u\frac{\partial c}{\partial x}+(\gamma-1)c\frac{\partial u}{\partial x}=0, \tag{7.42}$$

$$\frac{\partial u}{\partial t}+u\frac{\partial u}{\partial x}+\frac{2c}{\gamma-1}\frac{\partial c}{\partial x}=0. \tag{7.43}$$

If we now add or subtract appropriate multiples of these equations we obtain

$$\frac{\partial}{\partial t}\left(u\pm\frac{2c}{\gamma-1}\right)+(u\pm c)\frac{\partial}{\partial x}\left(u\pm\frac{2c}{\gamma-1}\right)=0. \tag{7.44}$$

By analogy with our analysis of the equations for one-dimensional traffic flow, we can see that the functions $R_\pm=u\pm 2c/(\gamma-1)$ are constant on the two sets of characteristic curves, $X_\pm(t)$, where

$$\frac{dX_\pm}{dt}=u\pm c. \tag{7.45}$$

Note that these are not necessarily straight lines. The functions $R_\pm(u,c)$ are called the **Riemann invariants** of the system. To summarise:

— On the C_+ characteristics, given by $dX_+/dt=u+c$, the C_+ invariant, $R_+=u+2c/(\gamma-1)$, is constant.
— On the C_- characteristics, given by $dX_-/dt=u-c$, the C_- invariant, $R_-=u-2c/(\gamma-1)$, is constant.

For the solution of a given initial value problem to be well-defined, a single C_+ characteristic and a single C_- characteristic must pass through each point in the domain of solution. The values of u and ρ at each point can then be determined from the initial values of $R_\pm$ on each characteristic.

We have already seen in section 7.1 how shock waves may develop in this type of system, but that not every mathematically plausible shock solution is physically correct. How can we extend these ideas to shock waves in ideal gases? One approach is to study the effect of viscosity and heat conduction in the neighbourhood of a shock. We will do this

in section 10.2 by using the method of multiple scales to determine the behaviour of a small disturbance of a uniform state. For general disturbances, it can be shown that characteristics must enter the shock locus, as we found in section 7.1 for shocks in traffic. An alternative but equivalent constraint is that *the entropy of a fluid particle must increase as it passes through a shock.* Outside the shock, we have seen that $DS/Dt = 0$, but the assumptions involved in the derivation of this equation break down at the shock. In particular, molecular diffusivities cannot be neglected at the shock, and entropy is generated there.

Example: The Generation of a Shock by a Uniformly Accelerating Piston. Consider an ideal gas confined in a long, straight cylinder by a tightly fitting piston, initially at rest at $x = 0$. In chapter 3, we showed how small amplitude oscillations of such a piston generate sound waves that propagate along the tube. We now consider the case where the gas and piston are initially at rest, and the piston moves into the gas with uniform acceleration a. The piston therefore lies at $x = \frac{1}{2}at^2$, and the gas in the region $x \geq \frac{1}{2}at^2$, initially with sound speed c_0, as shown in figure 7.22. We can anticipate some of what will happen here using linear theory. Combining $c_0^2 = \gamma/\rho$, and the equation of state $pV = RT$ we have c_0 proportional to $\sqrt{T}$. When the piston starts to compress the gas the temperature will rise. As this process continues the wave speed c_0 will rise and waves produced at later times will catch up with those produced earlier giving a multivaluedness to the solution. Let us now analyse this more quantitatively. We assume that the C_- characteristics that originate in the gas when $t = 0$ fill the domain. On these characteristics,

$$R_- = u - \frac{2c}{\gamma - 1} = -\frac{2c_0}{\gamma - 1},$$

and hence

$$c = c_0 + \frac{1}{2}(\gamma - 1)u,$$

throughout the gas. This also shows that all of the C_+ characteristics are straight lines, since on these, R_+, and hence u, c and dX_+/dt, are each constant. In particular, the C_+ characteristic that originates at the piston when $t = t_0$ satisfies

$$\frac{dX_+}{dt} = u + c = c_0 + \frac{1}{2}(\gamma + 1)at_0,$$

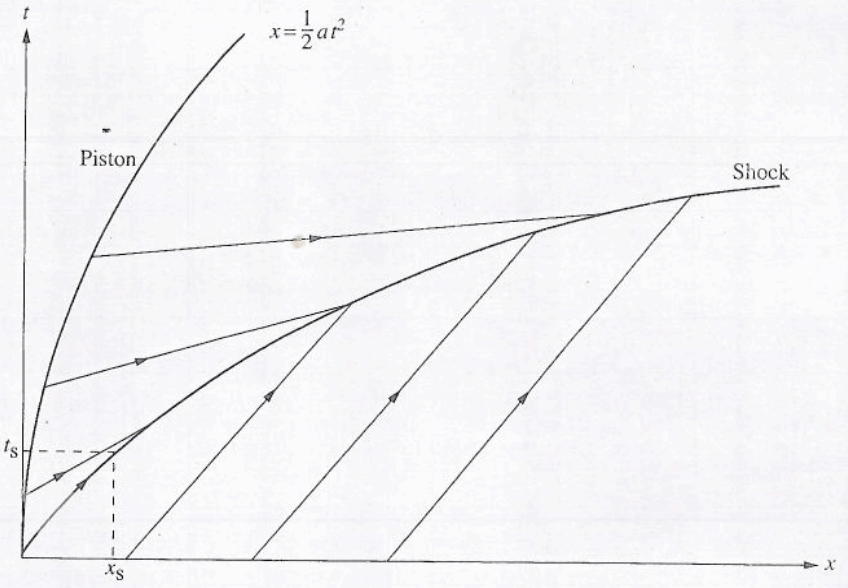

Fig. 7.22. The characteristics and shock path for the uniformly accelerating piston.

and hence

$$X_+(t;t_0) = \frac{1}{2}at_0^2 + \left\{c_0 + \frac{1}{2}(\gamma + 1)at_0\right\}(t - t_0).$$

The slopes of these straight lines increase with t_0, and we therefore expect them to intersect at some finite time t_s, when a shock forms, as shown in figure 7.22. As usual, we expect this to occur on neighbouring characteristics. For $\delta t_0 \ll 1$,

$$X_+(t, t_0 + \delta t_0) \approx X_+(t, t_0) + \delta t_0 \frac{\partial X_+}{\partial t_0}(t, t_0).$$

Neighbouring characteristics therefore intersect when $\partial X_+/\partial t_0 = 0$, and hence

$$t = \frac{2c_0}{a(\gamma + 1)} + \frac{2\gamma}{\gamma + 1}t_0.$$

This first occurs on the characteristic for which $t_0 = 0$, when

$$t = t_s = \frac{2c_0}{a(\gamma + 1)}, \quad x = x_s = \frac{2c_0^2}{a(\gamma + 1)}.$$

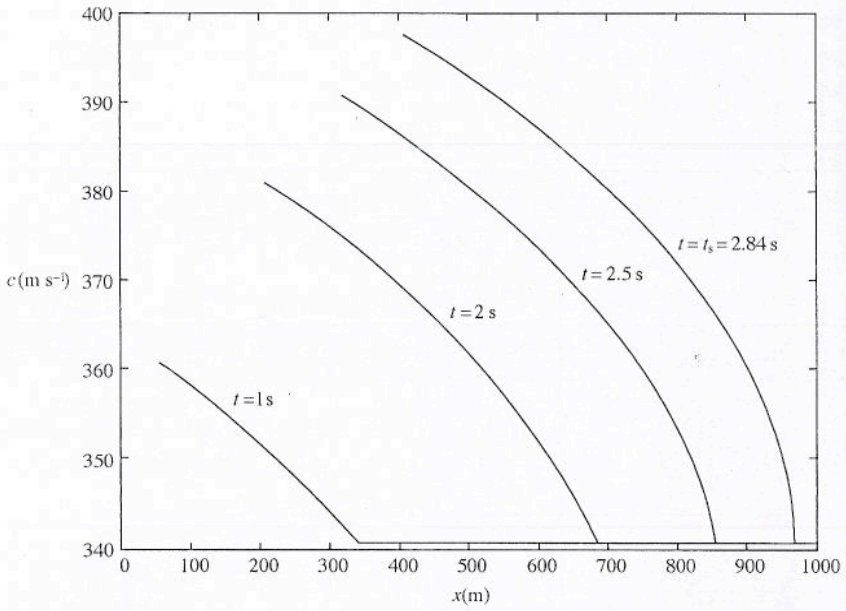

Fig. 7.23. The local sound speed when a piston accelerates at $100\,\mathrm{m\,s^{-2}}$ into a tube of air at atmospheric pressure and room temperature. A shock wave forms when $t = t_s \approx 2.84\,\mathrm{s}$ at $x = x_s \approx 969\,\mathrm{m}$. Note that the initial sound speed is $c_0 \approx 341\,\mathrm{m\,s^{-1}}$.

The gradual acceleration of the piston causes the wave that it generates to steepen until a shock wave forms in the body of the gas at $x = x_s$. This is illustrated in figure 7.23, which shows the local sound speed when the acceleration of the piston is $100\,\mathrm{m\,s^{-2}}$. The local sound speed increases behind the point $x = c_0 t$, until the gradient becomes infinite and a shock wave forms.

If the motion of the piston is started impulsively when $t = 0$, so that it lies at $x = Vt$ with $V > 0$, a shock forms immediately at the face of the piston (see subsection 8.1.1 for a qualitatively similar solution in the theory of shallow water waves).

For the shock waves that we have encountered so far in traffic flow, a simple application of conservation of cars sufficed to fix the position of the shock for $t > t_s$ through an application of the equal areas rule to the multi-valued solution obtained by the method of characteristics. The significant difference for shocks in gases is that, as we discussed above, the entropy of the gas changes across a shock. This means that once the shock has formed, the solution obtained using the method of

characteristics is no longer valid, since it was obtained on the assumption that the entropy of the gas is spatially uniform. A shock generates entropy in its wake.

In the next subsection, we determine what conditions must be satisfied at a shock in an ideal gas, and also demonstrate how the equal area rule can be resurrected when the shock wave is sufficiently weak.

7.2.4 The Rankine–Hugoniot Relations

We can learn a lot about how the various quantities change at a shock by considering the equations for conservation of mass, momentum and energy, (7.35), (7.36) and (7.37), in the neighbourhood of a shock. Assuming that the shock is planar and lies at $x = s(t)$, we can write (7.35) in integral form as

$$\frac{d}{dt}\int_{x_1}^{x_2} \rho dx + [\rho u]_{x_1}^{x_2} = 0. \tag{7.46}$$

We note that

$$\frac{d}{dt}\left(\int_{x_1}^{s(t)} + \int_{s(t)}^{x_2}\right)\rho dx = \left(\int_{x_1}^{s(t)} + \int_{s(t)}^{x_2}\right)\frac{\partial \rho}{\partial t}dx + \rho_R \dot{s} - \rho_L \dot{s},$$

where quantities immediately to the left and right of the shock are denoted by subscripts L and R. Taking the limits $x_1 \to s(t)$ and $x_2 \to s(t)$ in (7.46) then shows that

$$(\rho_L - \rho_R)\dot{s} = \rho_L u_L - \rho_R u_R.$$

If we define $\bar{u} = u - \dot{s}$, the velocity of the gas relative to the shock, we finally arrive at

$$\rho_L \bar{u}_L = \rho_R \bar{u}_R. \tag{7.47}$$

Similarly, (7.36) and (7.37) show that

$$\rho_L \bar{u}_L^2 + p_L = \rho_R \bar{u}_R^2 + p_R, \tag{7.48}$$

$$\left(\frac{1}{2}\rho_L \bar{u}_L^2 + \rho_L E_L + p_L\right)\bar{u}_L = \left(\frac{1}{2}\rho_R \bar{u}_R^2 + \rho_R E_R + p_R\right)\bar{u}_R. \tag{7.49}$$

These are known as the **Rankine–Hugoniot relations**, and express the fact that the flux of mass, momentum and energy must be continuous at a shock, whilst the pressure, density and internal energy of the gas may not be continuous. Figure 7.24 shows a planar shock in a frame of reference moving with the shock, with spatial coordinate $\bar{x} = x - \dot{s}$.

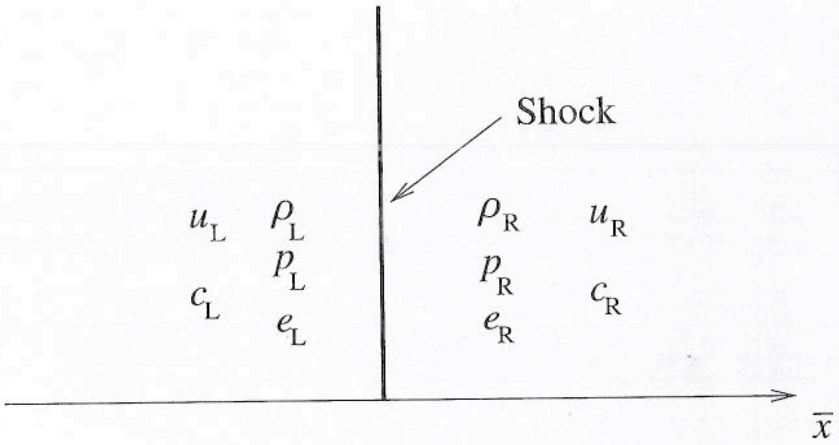

Fig. 7.24. The various physical quantities on either side of a planar shock.

For an ideal gas, $E = p/\rho(\gamma - 1)$, so the equation for continuity of the flux of energy, (7.49), can be written as

$$\left(\frac{1}{2}\bar{u}_L^2 + \frac{\gamma}{\gamma - 1}\frac{p_L}{\rho_L}\right)\rho_L\bar{u}_L = \left(\frac{1}{2}\bar{u}_R^2 + \frac{\gamma}{\gamma - 1}\frac{p_R}{\rho_R}\right)\rho_R\bar{u}_R.$$

Finally, using (7.47),

$$\frac{1}{2}\bar{u}_L^2 + \frac{\gamma}{\gamma - 1}\frac{p_L}{\rho_L} = \frac{1}{2}\bar{u}_R^2 + \frac{\gamma}{\gamma - 1}\frac{p_R}{\rho_R}. \tag{7.50}$$

The Rankine–Hugoniot relations can also be written in terms of the local sound speed, $c = \sqrt{\gamma p/\rho}$, as

$$\rho_L\bar{u}_L = \rho_R\bar{u}_R, \tag{7.51}$$

$$\rho_L\left(\bar{u}_L^2 + \frac{1}{\gamma}c_L^2\right) = \rho_R\left(\bar{u}_R^2 + \frac{1}{\gamma}c_R^2\right), \tag{7.52}$$

$$\frac{1}{2}\bar{u}_L^2 + \frac{1}{\gamma - 1}c_L^2 = \frac{1}{2}\bar{u}_R^2 + \frac{1}{\gamma - 1}c_R^2. \tag{7.53}$$

This is the usual form in which the Rankine–Hugoniot relations are written for an ideal gas.

Now that we have obtained (7.51), (7.52) and (7.53), what can we find out from them? Since these are three equations in six unknowns, $\bar{u}_L$, ρ_L, c_L, $\bar{u}_R$, ρ_R and c_R, we can always eliminate two of these and

obtain a single equation that involves any four unknowns. For example, to eliminate $\bar{u}_R$ and c_R, we use equation (7.51) to write

$$\bar{u}_R = \frac{\rho_L\bar{u}_L}{\rho_R}, \tag{7.54}$$

and (7.53) and (7.54) to write

$$c_R^2 = c_L^2 + \frac{1}{2}(\gamma - 1)\left(1 - \frac{\rho_L^2}{\rho_R^2}\right)\bar{u}_L^2, \tag{7.55}$$

If we now use (7.54) and (7.55) to eliminate $\bar{u}_R$ and c_R^2 from (7.52) we find that

$$\rho_L\left(1 - \frac{\rho_L}{\rho_R}\right)\bar{u}_L^2 + \frac{1}{\gamma}(\rho_L - \rho_R)c_L^2 = \rho_R\frac{\gamma - 1}{2\gamma}\left(1 - \frac{\rho_L^2}{\rho_R^2}\right)\bar{u}_L^2.$$

If we remove the factor of $(\rho_R - \rho_L)$, we obtain

$$\frac{\rho_L}{\rho_R}\bar{u}_L^2 - \frac{1}{\rho_R}\frac{\gamma - 1}{2\gamma}(\rho_R + \rho_L)\bar{u}_L^2 = \frac{1}{\gamma}c_L^2,$$

and a final rearrangement gives

$$(\gamma + 1)\frac{\rho_L}{\rho_R} = \gamma - 1 + \frac{2c_L^2}{\bar{u}_L^2}.$$

If we write this in terms of the local Mach number to the left of the shock, $M_L = \bar{u}_L/c_L$, we obtain

$$\frac{\rho_R}{\rho_L} = \frac{(\gamma + 1)M_L^2}{(\gamma - 1)M_L^2 + 2}.$$

It is most useful to write this equation in the final form

$$\frac{\rho_R}{\rho_L} = \frac{(\gamma - 1)M_L^2 + 2M_L^2}{(\gamma - 1)M_L^2 + 2}. \tag{7.56}$$

It is now clear that if $M_L^2 > 1$ then $\rho_R > \rho_L$, and vice versa. In other words, if the flow is locally supersonic ($M_L^2 > 1$), the density on that side of the shock is lower than it is on the other. By symmetry, we can deduce from (7.56) that

$$\frac{\rho_L}{\rho_R} = \frac{(\gamma - 1)M_R^2 + 2M_R^2}{(\gamma - 1)M_R^2 + 2}, \tag{7.57}$$

and hence that $M_L^2 > 1$ if and only if $M_R^2 < 1$. In other words, the flow must be supersonic on one side of the shock and subsonic on the other.

Many other deductions can be made from the Rankine–Hugoniot

relations using similar manipulations. In particular, the entropies on either side of a shock, S_L and S_R, satisfy (see exercise 7.6)

$$\frac{S_R - S_L}{c_V} = \log\left\{\frac{(1+z)\,(2\gamma+(\gamma-1)\,z)^{\gamma}}{(2\gamma+(\gamma+1)\,z)^{\gamma}}\right\}, \tag{7.58}$$

where $z = (p_R - p_L)/p_L$ is the **strength** of the shock. When $z \ll 1$, we say that the shock is **weak**. An expansion of (7.58) for $z \ll 1$ shows that

$$\frac{S_R - S_L}{c_V} \sim \frac{\gamma^2 - 1}{12\gamma^2} z^3. \tag{7.59}$$

This means that for sufficiently weak shocks very little entropy is generated. We will prove a similar result for the loss of energy across a shallow water bore in subsection 8.1.2. Figure 7.25 is a graph of (7.58), which shows that even when $z = 1$, $(S_R - S_L)/c_V \approx 0.01$, and the change in entropy is small. From (7.32), a small change in entropy across the shock leads to a small change in the gas law across the shock. This means that, for sufficiently weak shocks, to a good approximation we can assume that the flow remains isentropic and apply the equal area rule to the density predicted using the method of characteristics. This is the basis of **weak shock theory**, which we shall discuss in more detail in section 10.2.

Figure 7.26 shows a shock wave in air interacting with a sharp edge. The shock wave is generated using a shock tube and the air is at rest ahead of it. Behind the shock the pressure initially increases to 2.4 bar. From these measured quantities, the Rankine–Hugoniot relations give the density behind the shock as $1.8\,\mathrm{kg\,m^{-3}}$, the shock speed as $550\,\mathrm{m\,s^{-1}}$, and the gas velocity behind the shock as $250\,\mathrm{m\,s^{-1}}$.

Example: Reflection of a Shock Wave at a Planar, Solid Wall. As a final example of how the Rankine–Hugoniot relations can be used, let's consider the reflection of a shock wave that is incident normally on a planar, solid wall, as shown in figure 7.27. This is the approximate situation when the shock wave caused by an explosion hits a solid structure. We are particularly interested in the pressure at the wall immediately after the shock is reflected, since it is this that causes the force exerted on the solid structure. If the shock is incident at a significantly oblique angle, the situation is rather more difficult to analyse, and we do not consider this case here.

The first equation that we need, which comes from eliminating p_R and

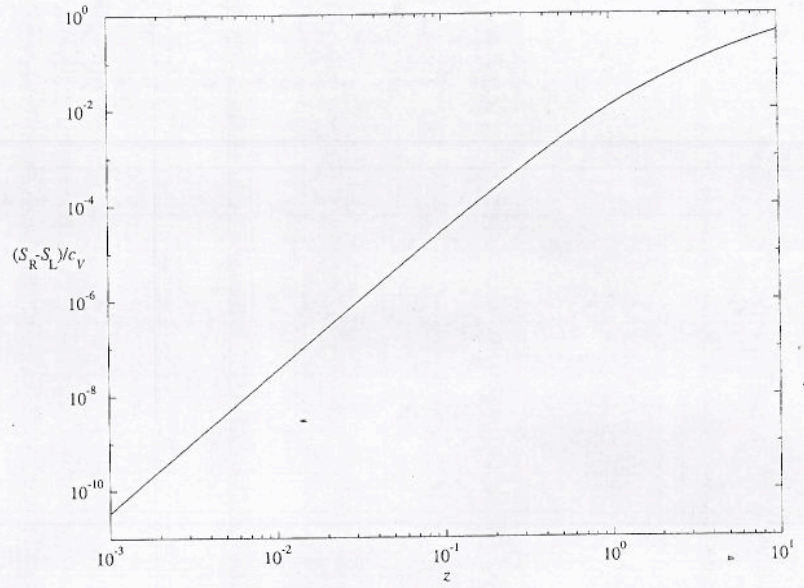

Fig. 7.25. The change in entropy across a shock of strength z.

ρ_R from (7.51) to (7.53), is (see exercise 7.5)

$$\left(\frac{2}{\gamma+1}\right)\bar{u}_L^2 + \bar{u}_L\,(\bar{u}_R - \bar{u}_L) - \left(\frac{2\gamma}{\gamma+1}\right)\frac{p_L}{\rho_L} = 0. \tag{7.60}$$

Just before the shock wave reaches the wall, propagating with velocity U_+, the gas pressure and density at the wall take the initial values p_0 and ρ_0. We also know that the normal velocity of the gas is zero at the wall. If the gas pressure, density and normal velocity behind the shock wave are p_s, ρ_s and u_s, we have $\bar{u}_L = u_s - U_+$ and $\bar{u}_R = -U_+$. Substituting this into (7.60) shows that

$$\left(\frac{2}{\gamma+1}\right)(u_s - U_+)^2 - u_s(u_s - U_+) - \left(\frac{2\gamma}{\gamma+1}\right)\frac{p_s}{\rho_s} = 0. \tag{7.61}$$

Immediately after the shock is reflected, its normal velocity is $-U_-$, and the gas pressure and density at the wall are the unknowns, p_1 and ρ_1. However, the normal velocity at the wall must still be zero. In addition, the gas pressure, density and velocity on the other side of the shock are still p_s, ρ_s and u_s, as shown in figure 7.27. This means that $\bar{u}_L = u_s + U_-$

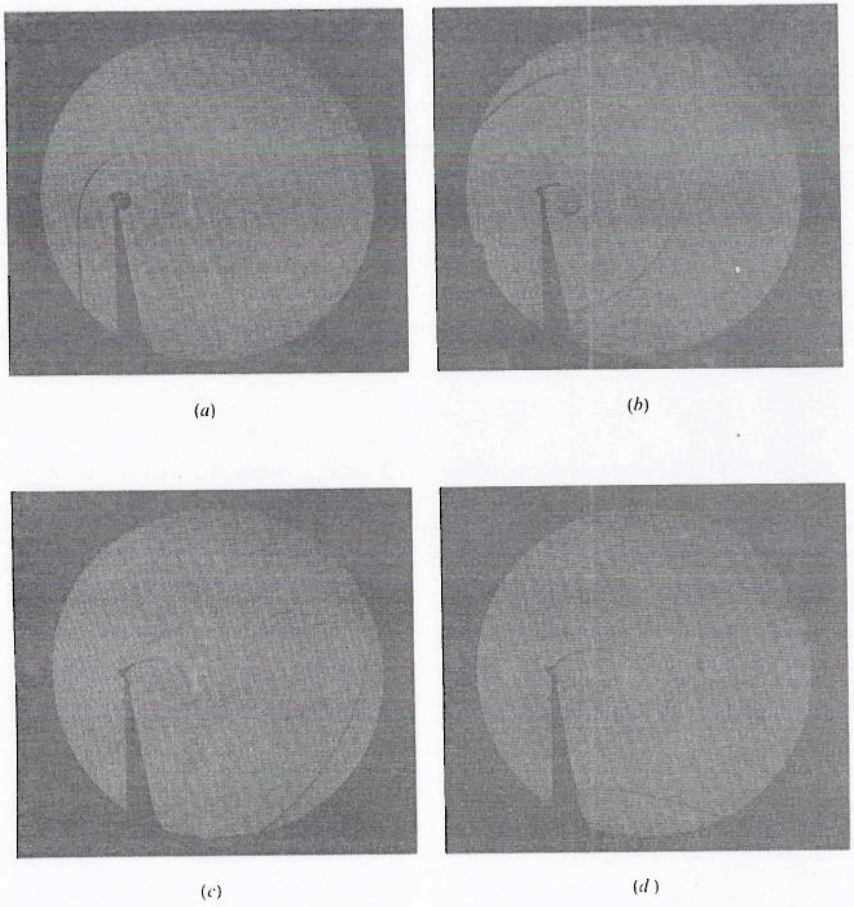

(a) (b) (c) (d)

Fig. 7.26. A shadowgraph photo of a shock interacting with a sharp edge.

and $\bar{u}_R = U_-$, so that

$$\left(\frac{2}{\gamma+1}\right)(u_s+U_-)^2 - u_s(u_s+U_-) - \left(\frac{2\gamma}{\gamma+1}\right)\frac{p_s}{\rho_s} = 0. \tag{7.62}$$

Comparing (7.61) and (7.62), we find that $u_s - U_+$ and $u_s + U_-$ satisfy the same quadratic equation, and must therefore be the two roots, whose product is

$$(u_s - U_+)(u_s + U_-) = -\frac{\gamma p_s}{\rho_s}. \tag{7.63}$$

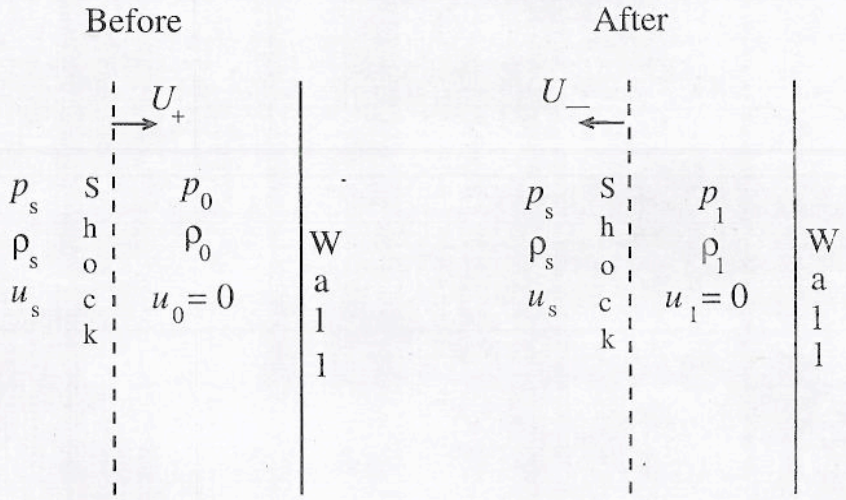

Fig. 7.27. The reflection of a shock wave incident normally on a solid wall.

The other equation that we need is

$$\left(\frac{2}{\gamma+1}\right)\frac{\rho_L \bar{u}_L^2}{p_L} = \frac{p_R}{p_L} + \frac{\gamma-1}{\gamma+1}, \tag{7.64}$$

which comes from (7.51) to (7.53) by eliminating $\bar{u}_R$ and ρ_R. From the values on either side of the shock before and after reflection, this implies that

$$\left(\frac{2}{\gamma+1}\right)\frac{\rho_L(u_s - U_+)^2}{p_L} = \frac{p_0}{p_s} + \frac{\gamma-1}{\gamma+1}, \tag{7.65}$$

$$\left(\frac{2}{\gamma+1}\right)\frac{\rho_L(u_s + U_-)^2}{p_L} = \frac{p_1}{p_s} + \frac{\gamma-1}{\gamma+1}. \tag{7.66}$$

If we now multiply these two equations together and use (7.63) to eliminate all the velocities, we find that

$$\left(\frac{p_0}{p_s} + \frac{\gamma-1}{\gamma+1}\right)\left(\frac{p_1}{p_s} + \frac{\gamma-1}{\gamma+1}\right) = \left(\frac{2\gamma}{\gamma+1}\right)^2. \tag{7.67}$$

Finally, when an explosion causes a shock wave to be incident on a wall, we expect that the pressure behind the shock wave will be much greater than that in front of it, so that $p_0 \ll p_s$. Using this approximation in

(7.67), we arrive at the strikingly simple result

$$\frac{p_1}{p_s} \approx \frac{3\gamma - 1}{\gamma - 1}. \tag{7.68}$$

For atmospheric air, with $\gamma \approx 1.4$, this gives $p_1 \approx 8p_s$. Not only does a solid structure, for example a bunker designed to protect its occupants from a conventional or nuclear blast, have to cope with the high pressure p_s incident upon it, the instantaneous pressure is magnified by a factor of eight by the dynamics of the reflection process.

7.2.5 Detonations*

When a shock wave passes through a gas, the temperature behind the shock is greater than that ahead of the shock. We can see this for an ideal gas by eliminating u_R and u_L from the Rankine–Hugoniot relations (7.51) to (7.53). The gas law shows that $p_R\rho_L/p_L\rho_R = T_R/T_L$, and leads to

$$\frac{T_R}{T_L} = \left\{ \frac{(\gamma+1)p_L + (\gamma-1)p_R}{(\gamma-1)p_L + (\gamma+1)p_R} \right\} \frac{p_R}{p_L}. \tag{7.69}$$

Simple calculus shows that the right hand side of this expression is a strictly increasing function of p_R/p_L, and hence that $T_R > T_L$ when $p_R > p_L$. For the shock shown in figure 7.26, the absolute temperature initially increases from about 20 °C to 110 °C. In the limiting case of a strong shock propagating from right to left, so that $p_R \gg p_L$ (see exercise 7.6),

$$\frac{T_R}{T_L} \sim \left(\frac{\gamma - 1}{\gamma + 1} \right) \frac{p_R}{p_L} \gg 1.$$

The stronger the shock, the greater the temperature increase.

If the gas through which the shock travels is combustible, for example a mixture of methane and air or hydrogen and air, the rise in temperature across the shock may be sufficient to initiate a chemical reaction and ignite the gas. Since the chemical reactions involved in combustion are extremely rapid, there are a region where the mixture of gases is burnt, and a region where the mixture is unburnt, separated by a thin **detonation wave**. We will assume that this wave is sufficiently thin relative to any geometrical length scales that we can model it as a surface of discontinuity, just as we did for a shock wave.

We can distinguish two different situations where a detonation wave can exist, in which, as we shall see below, it propagates in slightly

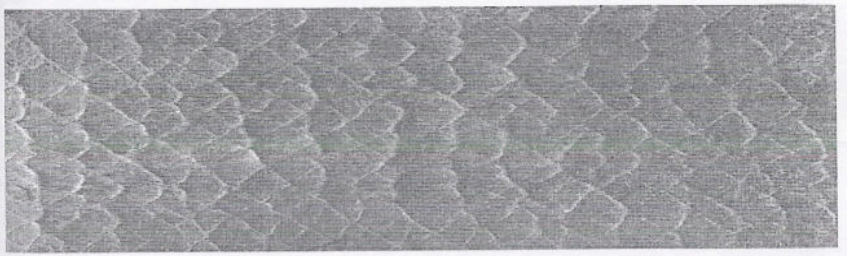

Fig. 7.28. Soot deposited on foil after a CJ detonation wave in a mixture of methane and oxygen has passed down a tube. The cellular pattern indicates that in this case the wave was laterally unstable.

different ways. Firstly, a shock wave may be incident on a combustible mixture and ignite it. Secondly, a combustible mixture may be ignited at a point by a local source of heat, such as a spark, and a detonation wave generated spontaneously by the violence of the chemical reaction. In the second situation, there is also the possibility of a **deflagration wave** propagating. These are rather similar to the chemical waves that we will study in chapter 9, where there is a balance between chemical reaction and diffusion of the heat generated. The dynamics of the compressible gas is of secondary importance in deflagration waves, and there is certainly no shock. The stability of deflagrations and detonations remains the subject of lively debate (for example, Brailovsky and Sivashinsky (1997), Sharpe and Falle (1999)). The effect of a passing detonation wave is shown in figure 7.28.

The Shock and Detonation Adiabatics and the Chapman–Jouguet Point

In order to investigate the propagation of detonation waves, it is first useful to consider the notion of the shock adiabatic for ordinary shock waves. Eliminating the gas temperature from (7.69) in favour of the gas density gives

$$\frac{p_R}{p_L} = \frac{(\gamma+1)\rho_L^{-1} - (\gamma-1)\rho_R^{-1}}{(\gamma+1)\rho_R^{-1} - (\gamma-1)\rho_L^{-1}}. \tag{7.70}$$

For given values of p_L and ρ_L^{-1}, this equation relates p_R to ρ_R^{-1} and is known as the **shock adiabatic**. It takes the form of a rectangular hyperbola, as plotted in figure 7.29. From the first two Rankine–Hugoniot relations,

$$j^2 = \frac{p_L - p_R}{\rho_R^{-1} - \rho_L^{-1}}, \tag{7.71}$$

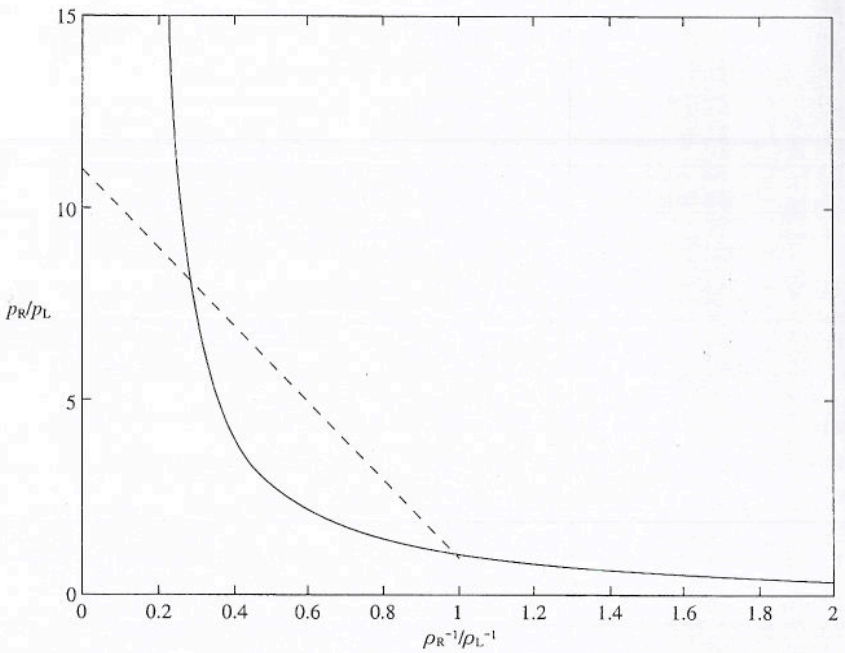

Fig. 7.29. The shock adiabatic for an ideal gas with $\gamma = 1.4$ (solid line), along with a typical straight line given by (7.71), (dashed line).

where $j = \rho_R \bar{u}_R = \rho_L \bar{u}_L$ is the flux of mass through the shock. If we consider the straight line joining the points (ρ_R^{-1}, p_R) and (ρ_L^{-1}, p_L) on the shock adiabatic, as shown in figure 7.29, its slope is therefore $-j^2$. We conclude that, for a given state (ρ_L^{-1}, p_L) ahead of the shock and a given mass flux j through the shock, the state of the gas behind the shock, (ρ_R^{-1}, p_R), can be determined graphically from the shock adiabatic by drawing a line of slope $-j^2$ through the point (ρ_L^{-1}, p_L). The other point of intersection will then give the final state, (ρ_R^{-1}, p_R).

For a detonation wave, the Rankine–Hugoniot relations in the form (7.47) and (7.48) still hold. The first modification to our analysis that we need to make for a detonation wave is to take into account the energy released by the chemical reaction in (7.49). The chemical reaction is confined to a thin region behind the shock wave, which we treat as a discontinuity in the internal energy of the gas. The second is to note that the ratio of specific heats may be different on each side of the detonation, since the chemical composition is different. The third Rankine–Hugoniot

relation (7.49) therefore becomes

$$\frac{1}{2}\bar{u}_R^2 + \frac{\gamma_R}{\gamma_R - 1}\frac{p_R}{\rho_R} = \frac{1}{2}\bar{u}_L^2 + \frac{\gamma_L}{\gamma_L - 1}\frac{p_L}{\rho_L} + q, \tag{7.72}$$

where q is the energy per unit mass released by the chemical reaction and γ_R and γ_L are the different specific heat ratios of the burnt and unburnt gases. If we now eliminate $\bar{u}_R$ and $\bar{u}_L$ from the Rankine–Hugoniot relations for the detonation we arrive at the equation of the **detonation adiabatic**,

$$\frac{\gamma_L + 1}{\gamma_L - 1}\frac{p_L}{\rho_L} - \frac{\gamma_R + 1}{\gamma_R - 1}\frac{p_R}{\rho_R} - \frac{p_L}{\rho_R} + \frac{p_R}{\rho_L} = -2q. \tag{7.73}$$

In contrast to the shock adiabatic, the detonation adiabatic does not pass through the initial point (p_L, ρ_L^{-1}). The shock and detonation adiabatics are shown in figure 7.30. The detonation adiabatic lies at a higher pressure for a given value of ρ^{-1} than the shock adiabatic because of the extra heat generated by the chemical reaction. However, (7.71) still holds, since it is derived from conservation of mass and momentum only. This means that the slope of the straight line from the initial state, (p_L, ρ_L^{-1}) to the final state, (p_R, ρ_R^{-1}), which now lies on the detonation adiabatic, is still $-j^2$. It is clear from figure 7.30 that there is now a lower bound on the value of j^2, corresponding to minus the slope of the detonation adiabatic at the point marked CJ, called the **Chapman–Jouguet point**, where the straight line (7.71) is tangent to it. Moreover, for j^2 greater than this minimum value, the line (7.71) meets the detonation adiabatic at two different points, B and C in figure 7.30. Only the state C corresponds to a physically realisable shock. We could deduce this from arguments involving entropy production at the detonation. There is, however, a simpler, physical argument.

The internal structure of the detonation, which we neglect in idealising it as a discontinuity, consists of a shock wave followed by a combustion region. Across the shock, the initial state of the gas changes to that given by the point D on the shock adiabatic, as shown in figure 7.30. Then, across the combustion region, the chemical reaction releases heat and the pressure of the gas decreases until it reaches the equilibrium state given by C on the detonation adiabatic. Thus the state C rather than the state B is reached across the detonation wave, simply because the associated shock heats the gas and precedes the combustion, not the other way around. We conclude that the set of possible states that the gas can reach across a detonation wave is given by the part of the detonation adiabatic lying above the CJ point.

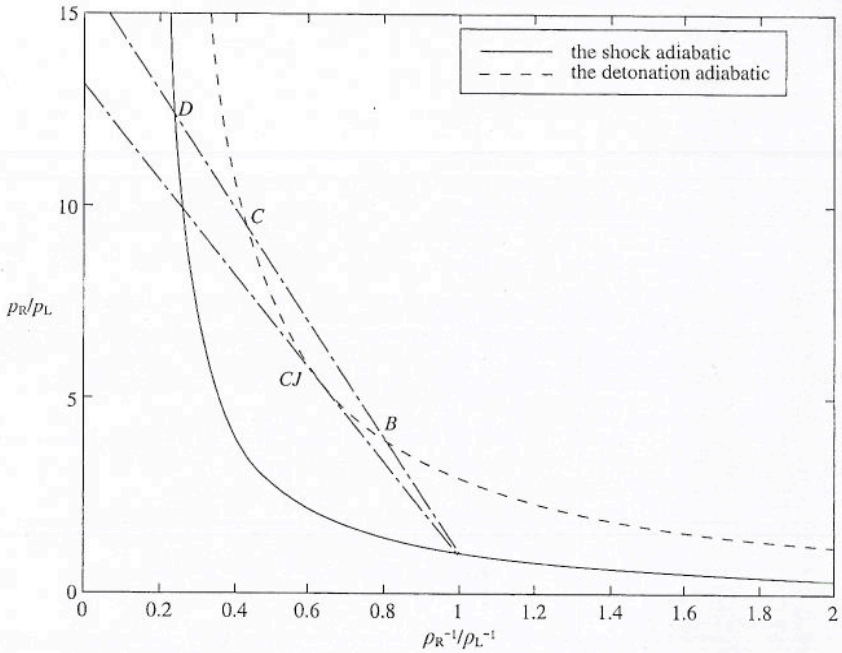

Fig. 7.30. The shock and detonation adiabatics for an ideal gas with $\gamma_R = \gamma_L = 1.4$, along with a typical straight line given by (7.71), which meets the detonation adiabatic at points B and C, and the unique line that meets the detonation adiabatic at the Chapman–Jouguet point CJ (dash–dotted lines).

At the CJ point, $dp_R/d\rho_R^{-1} = -j^2$. Since $dp_R/d\rho_R = c_R^2$ and $j^2 = \rho_R^2 \bar{u}_R^2$, this means that $\bar{u}_R = c_R$ at the CJ point. The detonation wave therefore moves at the local sound speed relative to the velocity of the burnt gas if its burnt state corresponds to the CJ point. This is not possible for a shock wave, since the line given by (7.71) can never be tangent to the shock adiabatic, as is clear from figures 7.29 and 7.30. We can also note that on the part of the detonation adiabatic that lies above the CJ point, for example point C in figure 7.30, $-j^2 > dp_R/d\rho_R^{-1} = -\rho_R^2 c_R^2$, and hence $\bar{u}_R < c_R$. We conclude that, in general, a detonation wave moves at or below the speed of sound relative to the burnt gases behind it, and that the uniquely determined detonation that moves at the local speed of sound corresponds to the Chapman–Jouguet point, CJ, on the detonation adiabatic, and hence the lowest possible pressure and density in the burnt gases.

When a shock wave is incident on a combustible gas and becomes a detonation wave, the strength of the detonation depends on the strength

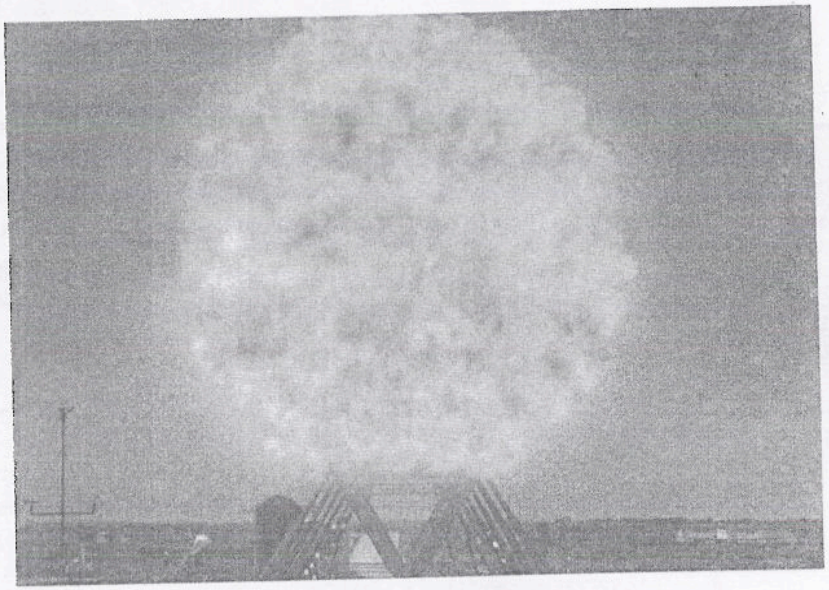

Fig. 7.31. A spherical detonation wave initiated using high explosives.

of the incident shock, and the state of the burnt gases can lie anywhere on the detonation adiabatic above the CJ point. We say that the detonation may be **over-driven** (see exercise 7.8). However, when a detonation wave is ignited from within a combustible mixture by some local source of heating, it usually corresponds to the CJ point. As an example of this, we will consider the propagation of a spherical detonation wave away from its point of ignition. This has some relevance to the behaviour of supernovas (for example, Wiggins, Sharpe and Falle (1998)).

Example: a Spherical Detonation Wave. Figure 7.31 shows a spherical detonation wave, initiated using high explosives. Let's see if we can describe such a wave mathematically. In spherical polar coordinates, the equations for conservation of mass momentum and energy for a spherically symmetric flow are

$$\frac{\partial \rho}{\partial t} + \frac{\partial (\rho u)}{\partial r} + \frac{2\rho u}{r} = 0, \tag{7.74}$$

$$\frac{\partial u}{\partial t} + u\frac{\partial u}{\partial r} = -\frac{1}{\rho}\frac{\partial p}{\partial r}, \tag{7.75}$$

$$\frac{\partial S}{\partial t} + u\frac{\partial S}{\partial r} = 0. \tag{7.76}$$

For a detonation wave generated at a point, there is no geometrical length scale, and the only parameters in the problem are p_0 and ρ_0, the initial pressure and density in the unburnt gases, and q, the heat generated by the chemical reaction. We can form just two dimensionless groups involving r and t, namely $\rho_0 r^2/p_0 t^2$ and r^2/qt^2. We conclude that the solution will be of similarity form, with all the dependent variables functions of $\eta = r/t$. We need to solve (7.74) to (7.76) for $0 \leq \eta < \eta_0$, with a detonation at $\eta = \eta_0$ and the gas at rest in its unburnt state for $\eta > \eta_0$.

If we write $\rho \equiv \rho(\eta)$, $u \equiv u(\eta)$ and $p \equiv p(\eta)$, (7.76) becomes

$$(u - \eta)\, S' = 0, \tag{7.77}$$

where a prime denotes $d/d\eta$. Provided that $u \neq \eta$, which we shall see below does not occur, the entropy S must be a constant behind the spherical detonation wave. We therefore have $p' = c^2\rho'$, and can eliminate p and ρ between (7.74) and (7.75) to obtain

$$u' = \frac{2u}{\eta}\left\{\frac{(u-\eta)^2}{c^2} - 1\right\}^{-1} \qquad c' = -(\gamma - 1)\frac{u(u-\eta)}{c\eta}\left\{\frac{(u-\eta)^2}{c^2} - 1\right\}^{-1}. \tag{7.78}$$

These nonlinear ordinary differential equations determine how the gas velocity u and local sound speed c vary behind the detonation wave. We can write (7.78) in dimensionless form by defining

$$X = \frac{\eta}{c_0}, \quad U = \frac{u}{c_0}, \quad C = \frac{c}{c_0}$$

which gives

$$\frac{dU}{dX} = \frac{2U}{X\{(U-X)^2 - 1\}}, \quad \frac{dC}{dX} = -\frac{(\gamma-1)CU(U-X)}{X\{(U-X)^2-1\}}. \tag{7.79}$$

Since there are no sources of mass, the gas velocity must be zero at $X = 0$, and it is helpful to consider the solution when $U \ll 1, C \sim 1$. Provided X is not close to one, (7.79) gives at leading order

$$\frac{dU}{dX} = \frac{2U}{X(X^2-1)}. \tag{7.80}$$

We can solve this separable equation and obtain

$$U = k\left(1 - \frac{1}{X^2}\right), \tag{7.81}$$

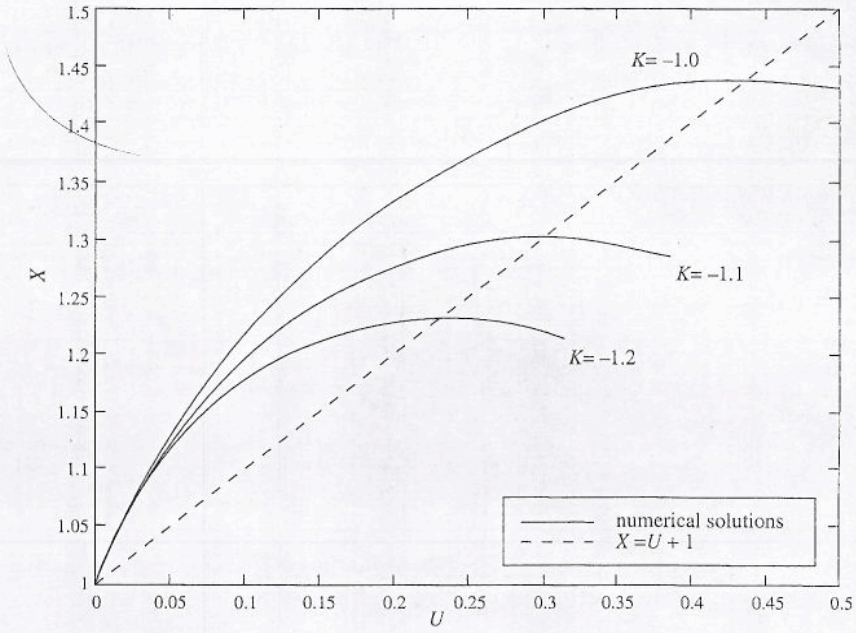

Fig. 7.32. Numerical solutions of (7.83) for various values of K.

where k is a constant. Since $U \to 0$ as $X \to 1$, we cannot in fact assume that X is not close to one, and this solution is not valid. We have therefore shown that U can only be small in the neighbourhood of $X = 1$. To proceed, we define $\hat{X} = X - 1, \hat{C} = C - 1$, and seek a solution for $U, \hat{C}$ and $\hat{X}$ small. At leading order

$$\frac{dU}{d\hat{X}} = \frac{U}{\hat{X} - U}, \quad \frac{d\hat{C}}{d\hat{X}} = \frac{1}{2}(\gamma - 1)\frac{U}{\hat{X} - U - \hat{C}}. \tag{7.82}$$

This equation is linear in $\hat{X}$, and has the implicit solution

$$\hat{X} = KU - \tfrac{1}{2}(\gamma+1)U\log U, \quad \hat{C} \sim \tfrac{1}{2}(\gamma-1)U,$$

which gives

$$X \sim 1 - \tfrac{1}{2}(\gamma+1)U\log U + KU, \quad C \sim 1 + \tfrac{1}{2}(\gamma-1)U, \quad \text{as } U \to 0, \tag{7.83}$$

for some constant K. This shows that $U \to 0$ and $dU/dX \to 0$ as $X \to 1^+$. We conclude that the solution has $U = 0, C = 1$ for $0 \leq X \leq 1$, with U and C given implicitly by (7.83) for $(X - 1)$ small and positive. We now need to consider how U and C behave for $X > 1$. Before doing this, let's consider where a detonation wave can exist. For $X > U + C$,

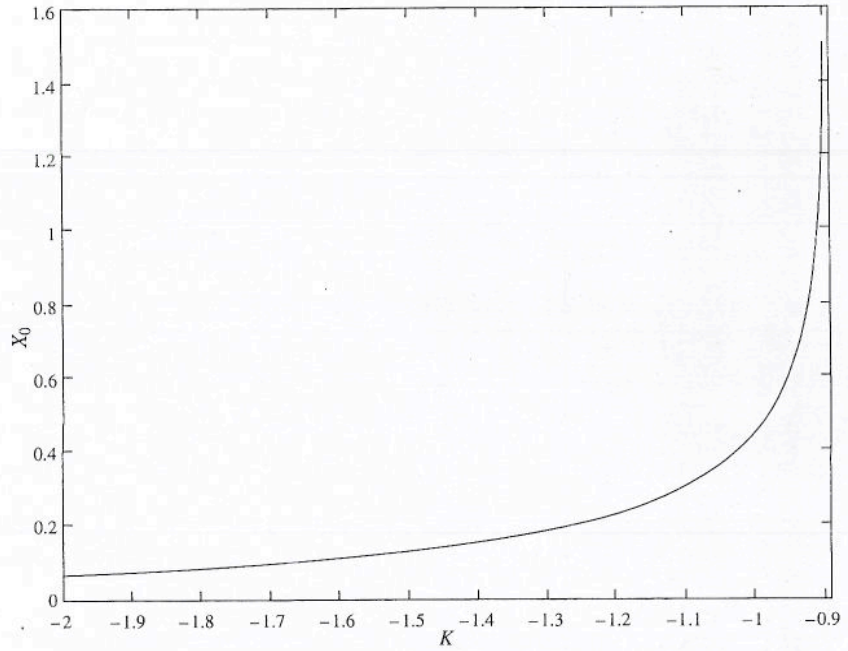

Fig. 7.33. The position at which dU/dX becomes infinite as a function of K.

in terms of the physical variables, $r > ut + ct$. If the detonation wave lies at $r = r_0(t)$ with $r_0(t) > ut + ct$, the local speed of sound is less than the velocity of the burnt gas relative to the speed of the shock. We have already seen that this is not physically possible, and we therefore need to insert the detonation at some point where $X \leq U + C$.

It is rather easier to treat X and C as functions of U. Some numerical solutions of (7.79) are shown in figure 7.32 using (7.83) to begin the integration at $X = 1 + \epsilon$ with $\epsilon \ll 1$ for various values of K. From (7.79) we can see that $dX/dU = 0$ when $X = U \pm C$. Each of the solutions shown in figure 7.32 has $X > U + C$ until it meets the line $X = U + C$ at $X = X_0$, where it has a local maximum. Treating these solutions as giving U as a function of X, they are valid for $1 \leq X \leq X_0$, at which point dU/dX becomes unbounded. Numerical integration of (7.79) suggest that such solutions exist for each $K < K_0$, with $K_0 \approx -2.1$. For $K > K_0$, X becomes unbounded at a finite value of U, and does not provide a solution appropriate to a detonation, since $X > U + C$. The function $X_0(K)$ is plotted in figure 7.33 for $K < K_0$.

To complete the solution, we must insert a detonation wave at $X = X_0$,

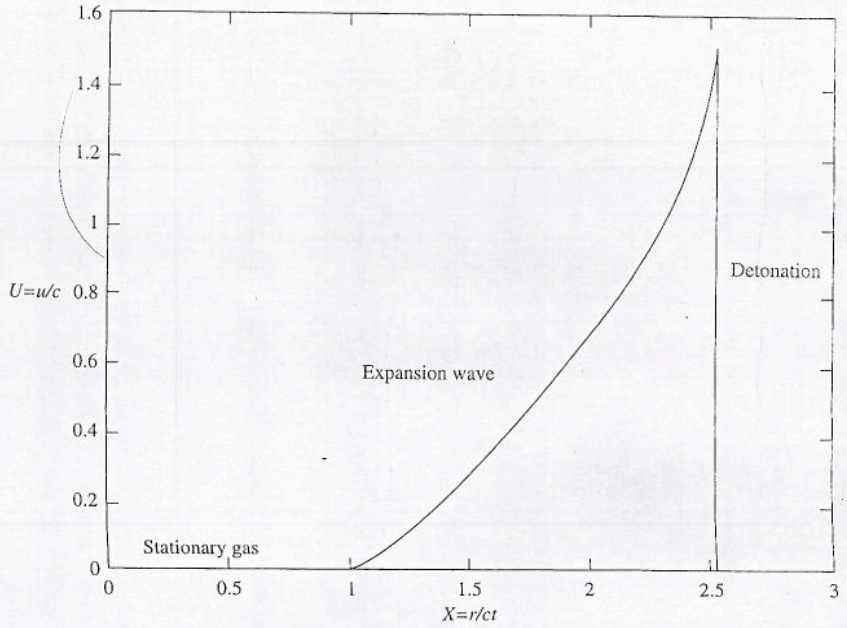

Fig. 7.34. A typical similarity solution for a spherical detonation.

across which U falls to zero, its initial value. This gives a family of solutions with $U = 0$ for $X \leq 1$ and $X \geq X_0(K)$, and U monotonically increasing for $1 \leq X \leq X_0(K)$. A typical solution is shown in figure 7.34. However, at $X = X_0$, $X = U + C$, and hence $u = X_0c_0 - c$. Since, the detonation lies at $r = r_0 = X_0c_0t$ and therefore moves with speed X_0c_0, we conclude that the burnt gases behind the detonation move at the local sound speed relative to the detonation, and hence that the detonation corresponds to the CJ point on the detonation adiabatic. For a mixture of gases, this CJ detonation is associated with a unique value of u, the velocity of the burnt gases behind the detonation, and hence a unique value of X_0. The appropriate similarity solution is therefore selected by the Rankine–Hugoniot conditions at the detonation, in particular, by the amount of heat generated by the chemical reaction.

Physically, we can see that the solution consists of a stationary sphere of gas of radius c_0t centred on the point of ignition, $r = 0$, connected to a spherical Chapman–Jouguet detonation at $r = X_0c_0t$ by an expansion wave across which u increases continuously from zero to $X_0c_0 - c$.

Exercises

7.1 The flow of traffic along a single lane road is modelled using

$$\frac{\partial \rho}{\partial t} + \frac{\partial}{\partial t}(\rho v(\rho)) = 0,$$

where $\rho(x,t)$ is the density of cars and $v(\rho)$ their velocity. If $v(\rho) = v_0(\rho_{\max} - \rho)/\rho_{\max}$ and

(a) $\rho(x,0) = \begin{cases} 0 & \text{for } x \le 0, \\ \rho_1 x^2/L^2 & \text{for } 0 \le x \le L, \\ \rho_1 & \text{for } x \ge L, \end{cases}$

(b) $\rho(x,0) = \rho_1 \exp(-k|x|)$,

where L, k and $\rho_1 \le \rho_{\max}$ are positive constants, determine when and where the solution first becomes undefined and hence a shock forms in each case. Sketch the solutions up to the development of the shock. Use the equal areas rule to make sketches of the progress of the shock in each case.

7.2 Using the model given in the previous exercise, the initial car density is

$$\rho(x,0) = \rho_0 + H(\pi - |bx|)\, a \sin bx,$$

where ρ_0, a and b are constants, with $\rho_0 > 0$, $|a| < \rho_0$ and $\rho_0 + |a| < \rho_{\max}$, and H is the Heaviside step function.

Show that when ab is positive, a single shock wave forms at time $t = \rho_{\max}/2v_0|ab|$, and that if ab is negative, two shock waves are formed simultaneously, again at time $t = \rho_{\max}/2v_0|ab|$. In each case, where are the shock waves when they form?

By fitting appropriate shocks to the multi-valued solution in each case, show that for $t \gg 1$ the maximum value of ρ is approximately

$$\rho_0 + \frac{\pi \rho_{\max}}{2v_0|b|t}$$

when ab is positive, and

$$\rho_0 + \sqrt{\frac{-2\rho_{\max} a}{v_0 b t}}$$

when ab is negative.

7.3 The flow of cars along a single lane road can be described using a continuous car density, $\rho(x,t)$, with car velocity given by

$$v(\rho) = \frac{v_0}{\rho_{\max}^2}(\rho_{\max} - \rho)^2,$$

for $0 \le \rho \le \rho_{\max}$. Write down the equation satisfied by ρ, and determine the kinematic wave speed, $c(\rho)$. Show that $c(\rho)$ is zero at $\rho = \frac{1}{3}\rho_{\max}$ and has a minimum at $\rho = \frac{2}{3}\rho_{\max}$.

At time $t = 0$, the car density is

$$\rho(x,0) = \frac{\rho_L + \rho_R e^{x/L}}{1 + e^{x/L}},$$

with $0 < \rho_R < \frac{1}{3}\rho_{\max}$ and $\frac{2}{3}\rho_{\max} < \rho_L < \rho_{\max}$. Sketch the function $c(\rho(x,0))$. Sketch the development of the car density for $t > 0$. How does this solution differ from the solution with $v(\rho) = v_0(\rho_{\max} - \rho)/\rho_{\max}$?

By considering the limit $L \to 0$, show that the car density changes discontinuously from ρ_L to $\rho_{\max} - \rho_L/2$ at a shock wave, which propagates with velocity $c(\rho_{\max} - \rho_L/2)$.

7.4 A piston confines a ideal gas within a semi-infinite tube of uniform cross-section. When $t = 0$ the gas is at rest and has sound speed c_0. For $t \ge 0$:

(a) The piston moves with a constant velocity $-V$ with $V > 0$. Show that the solution takes the form of an expansion fan and determine the solution.

(b) The piston moves with velocity $A\omega \sin \omega t$, where A and ω are positive constants. Show that a shock wave first forms when $t = t_s = 2c_0/A\omega^2(\gamma + 1)$.

7.5 Derive (7.60) and (7.64) from the Rankine–Hugoniot relations.

7.6 A plane shock wave is propagating in an ideal gas with ratio of specific heats γ. In a frame of reference where the shock is stationary at $x = 0$, the sound speed, gas pressure, density and velocity are given by c_R, p_R, ρ_R and $\bar{u}_R$ for $x > 0$, and c_L, p_L, ρ_L and $\bar{u}_L$ for $x < 0$. In addition, $\bar{u}_L > 0$, so the gas passes from left to right through the shock. Use the Rankine–Hugoniot relations to show that

$$z = \frac{2\gamma(M_L^2 - 1)}{\gamma + 1}, \tag{7.84}$$

$$\frac{\rho_R}{\rho_L} = \frac{2\gamma + (\gamma + 1)z}{2\gamma + (\gamma - 1)z}, \tag{7.85}$$

$$\frac{S_R - S_L}{c_V} = \log\left\{\frac{(1+z)(2\gamma + (\gamma - 1)z)^\gamma}{(2\gamma + (\gamma + 1)z)^\gamma}\right\}, \tag{7.86}$$

where $z = (p_R - p_L)/p_L$, $M_L = \bar{u}_L^2/c_L^2$, S_L and S_R are the entropies on either side of the shock, and c_V is the specific heat of the gas at constant volume.

Using (7.86), show that $d(S_R - S_L)/dz > 0$ for $\gamma > 1$ and $z > -1$, and hence that for the entropy of the gas to increase as it passes through the shock, $z > 0$. Now use (7.84) and (7.85) to show that $\rho_R > \rho_L$, and that the flow is subsonic for $x > 0$ and supersonic for $x < 0$.

7.7 A strong detonation wave is normally incident upon a rigid plane wall. What is the pressure at the wall after the detonation is reflected?

7.8 A piston initially at $x = 0$ confines an ideal combustible mixture of gases in a straight, semi-infinite tube lying in $x > 0$. When $t = 0$ the piston moves into the tube at speed $V > 0$. If a detonation wave forms immediately, show that an over-driven detonation is formed if $V > V_0$ and determine V_0.

8

Nonlinear Water Waves

We begin our examination of nonlinear water waves by studying the nonlinear shallow water equations. We looked at the linearised version of these equations in chapter 4. The nonlinear equations are closely related to those that we studied in chapter 7, and there is the possibility of shock, or bore, formation. We then consider the effect of nonlinearity on deep water, progressive gravity waves, determining in particular how the wave speed and waveform depend upon the small amplitude of the wave. When the competing effects of linear dispersion and nonlinear wave steepening act in a shallow water flow, we will show that the **Korteweg–de Vries equation** can control the leading order behaviour of the waves. In the final section, we consider nonlinear capillary waves in deep water, and demonstrate how complex variable theory can be used to derive analytical solutions.

8.1 Nonlinear Shallow Water Waves

In section 4.7 we derived the equations, (4.80) and (4.81), that govern the flow of shallow water, where the horizontal wavelength of disturbances is much greater than the vertical depth. For shallow water flowing over a horizontal bed, with $h_0(x)$ constant, these equations become

$$\frac{\partial h}{\partial t} + u\frac{\partial h}{\partial x} + h\frac{\partial u}{\partial x} = 0, \tag{8.1}$$

$$\frac{\partial u}{\partial t} + u\frac{\partial u}{\partial x} + g\frac{\partial h}{\partial x} = 0, \tag{8.2}$$

where u is the horizontal velocity and h the vertical depth. We have already looked at the linearised version of these equations. We now wish to study the full nonlinear equations.